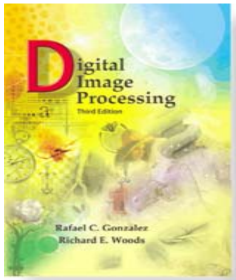

Digital Image Processing, 3rd ed.

Gonzalez & Woods

www.ImageProcessingPlace.com

Chapter 4
Filtering in the Frequency Domain

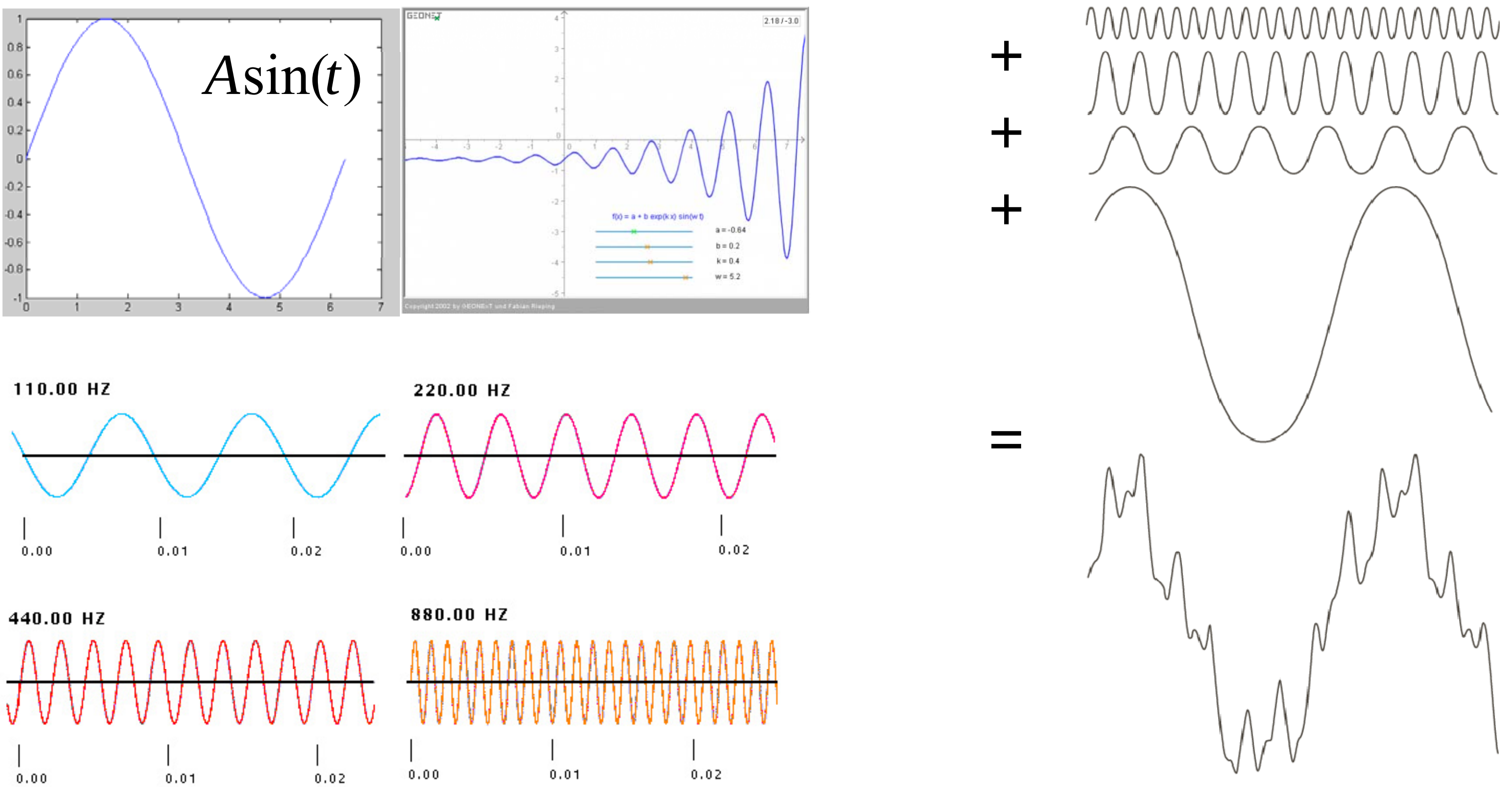

© 1992–2008 R. C. Gonzalez & R. E. Woods

Step Function

The unit step function, is a discontinuous function whose value is zero for negative argument and one for positive argument.

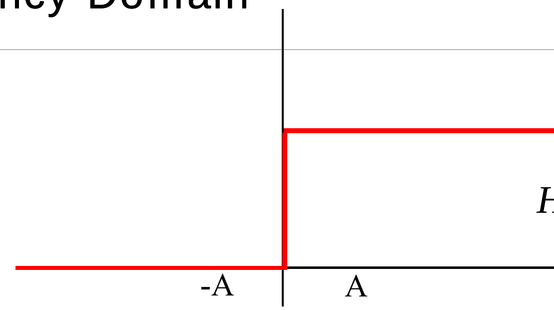

$$H(t)=\begin{cases}0 & t<0\\ 0 & t\geq 0\end{cases}$$

Rectangle Function

The unit step function, is a discontinuous function whose value is zero for negative argument and one for positive argument.

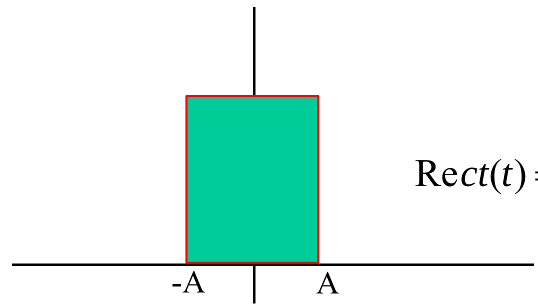

$$\mathrm{Rect}(t)=\begin{cases}0 & t>A\\ 1 & -A\leq t\leq A\\ 0 & t<-A\end{cases}$$

Impulse Function

The Dirac delta function, or δ function, is zero for all values of the parameter except when the parameter is zero, and its integral over the parameter from $-\infty$ to ∞ is equal to one

$$\int_{-\infty}^{\infty}\delta(t)dt=1$$

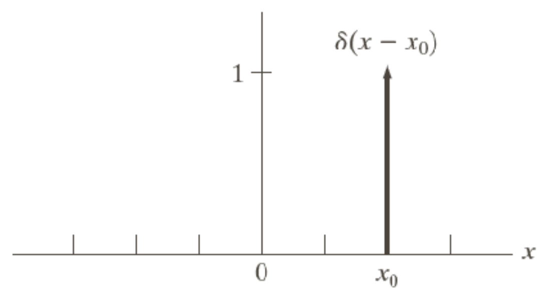

$$\delta(t)=\begin{cases}\infty & t=0\\ 0 & t\neq 0\end{cases}$$

© 1992–2008 R. C. Gonzalez & R. E. Woods

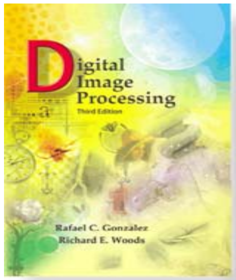

$$\int_{-\infty}^{\infty} f(t)\delta(t)dt = f(0)$$

$$\int_{-\infty}^{\infty} f(t)\delta(t-t_0)dt = f(t_0)$$

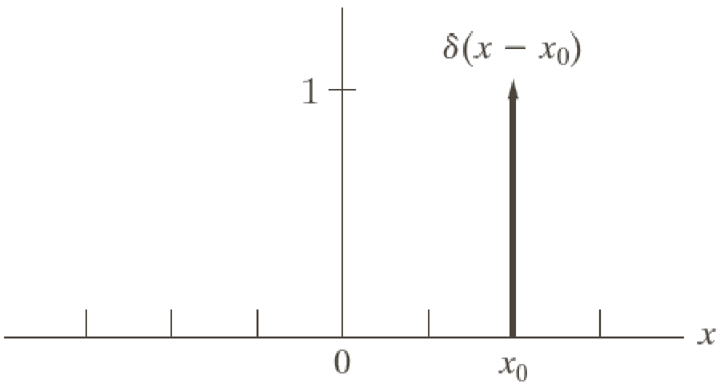

In discrete variable

$$\delta(x) = \begin{cases} 1 & x = 0 \\ 0 & t \neq 0 \end{cases}$$

$$\sum_{x=-\infty}^{\infty} f(x)\delta(x) = f(0)$$

$$\sum_{x=-\infty}^{\infty} f(x)\delta(x-x_0) = f(t_0)$$

© 1992–2008 R. C. Gonzalez & R. E. Woods

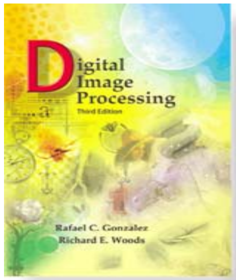

$$s_{\Delta T}(t)=\sum_{n=-\infty}^{\infty}\delta(t-n\Delta T)$$

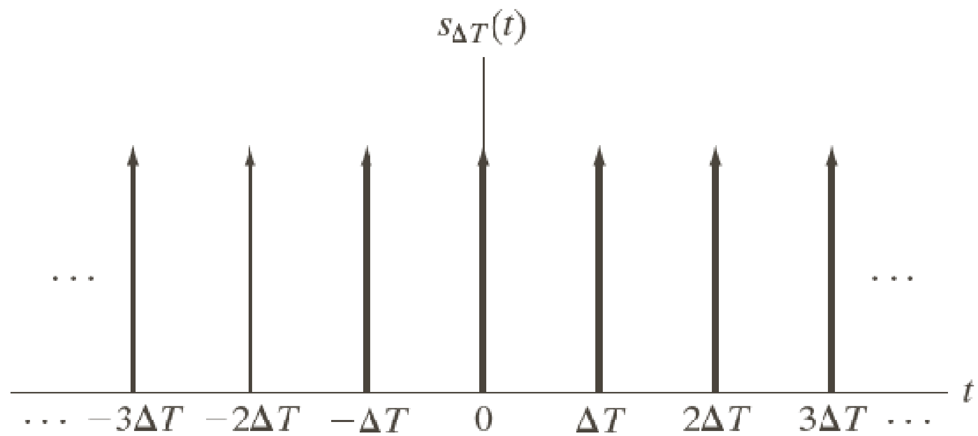

© 1992–2008 R. C. Gonzalez & R. E. Woods

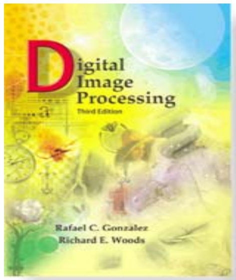

Complex Number

$$j^2 = -1$$

$$C = R + jI$$

$$\overline{C} = R - jI$$

$$|C| = \sqrt{R^2 + I^2}$$

$$\tan(\theta) = \frac{I}{R}$$

$$C = |C|(\cos(\theta) + j\sin(\theta))$$

$$e^{j\theta} = \cos(\theta) + j\sin(\theta)$$

© 1992–2008 R. C. Gonzalez & R. E. Woods

Function Representation

- Taylor Series

$$f(x)=\sum_{n=0}^{\infty}\frac{1}{n!}f^{(n)}(x_0)\cdot(x-x_0)^n$$

$$e^x=1+\frac{x}{1!}+\frac{x^2}{2!}+\frac{x^3}{3!}+\frac{x^4}{4!}+\ldots+\frac{x^n}{n!}+\ldots$$

- Fourier Series

$$f(t)=\frac{a_0}{2}+\sum_{n=1}^{\infty}(a_n\cos(nt)+b_n\sin(nt))$$

$$f(t)=\frac{2k}{\pi^3}[\sin(\pi t/k)-\tfrac{1}{2}\sin(2\pi t/k)+\tfrac{1}{3}\sin(2\pi t/k)-..];0<t<k$$

© 1992–2008 R. C. Gonzalez & R. E. Woods

$$e^x$$

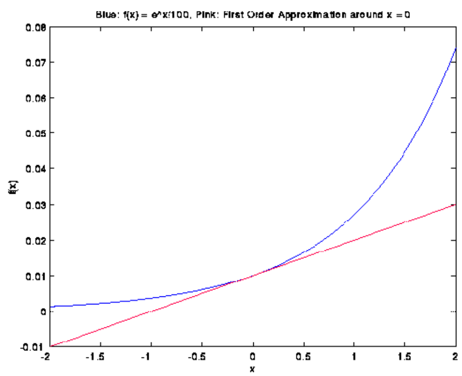

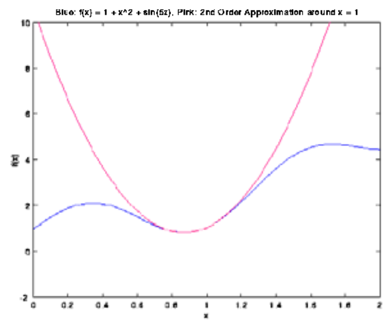

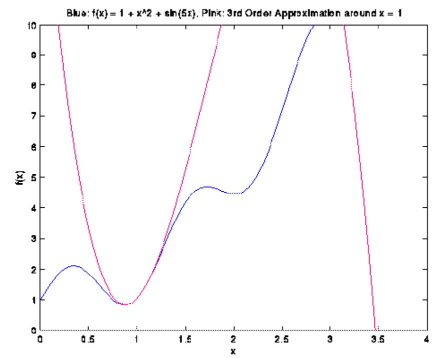

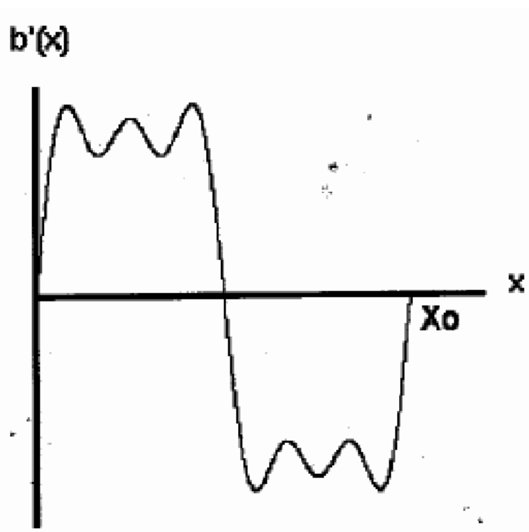

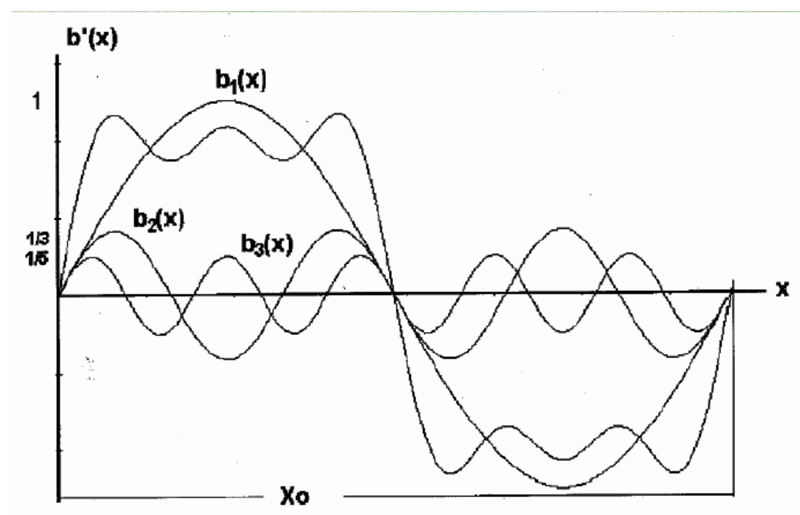

© 1992–2008 R. C. Gonzalez & R. E. Woods

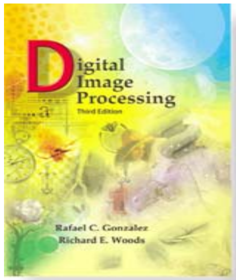

Fourier Transform

For a give function *g(x)* of a real variable x, the Fourier transformation of *g(x)* which is denoted as

$$\Im\{\mathrm{g(x)}\} = \mathrm{G(u)} = \int_{-\infty}^{\infty} g(x) e^{-j2\pi ux} dx$$

$$\Im^{-1}\{\mathrm{g(x)}\} = \mathrm{G(u)} = \int_{-\infty}^{\infty} g(x) e^{j2\pi ux} dx$$

© 1992–2008 R. C. Gonzalez & R. E. Woods

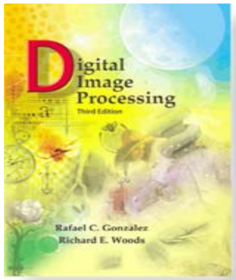

Since

$$e^{-j2\pi t} = \sin(2\pi t) - j\cos(2\pi t)$$

For that reason the Fourier transform F(u)

$F(u) = R(u) + jI(u)$

Which often appear as

$$F(u) = |F(u)|\, e^{j\phi(u)}$$

$$|F(u)| = \sqrt{R(u)^2 + I(u)^2}$$

$$\tan(\phi(u)) = \frac{I(u)}{R(u)}$$

© 1992–2008 R. C. Gonzalez & R. E. Woods

Spatial Domain

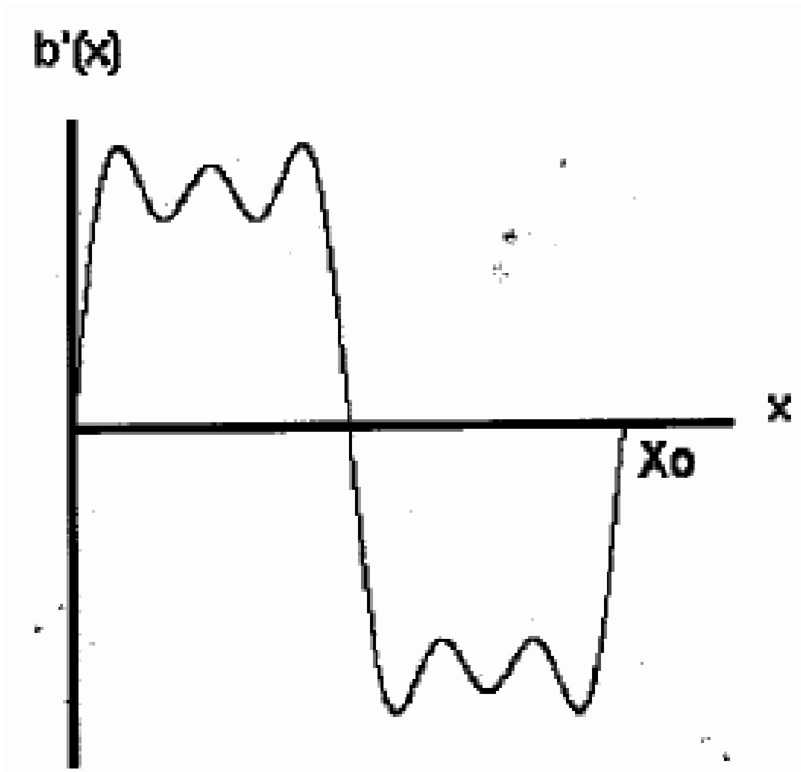

Frequency Domain

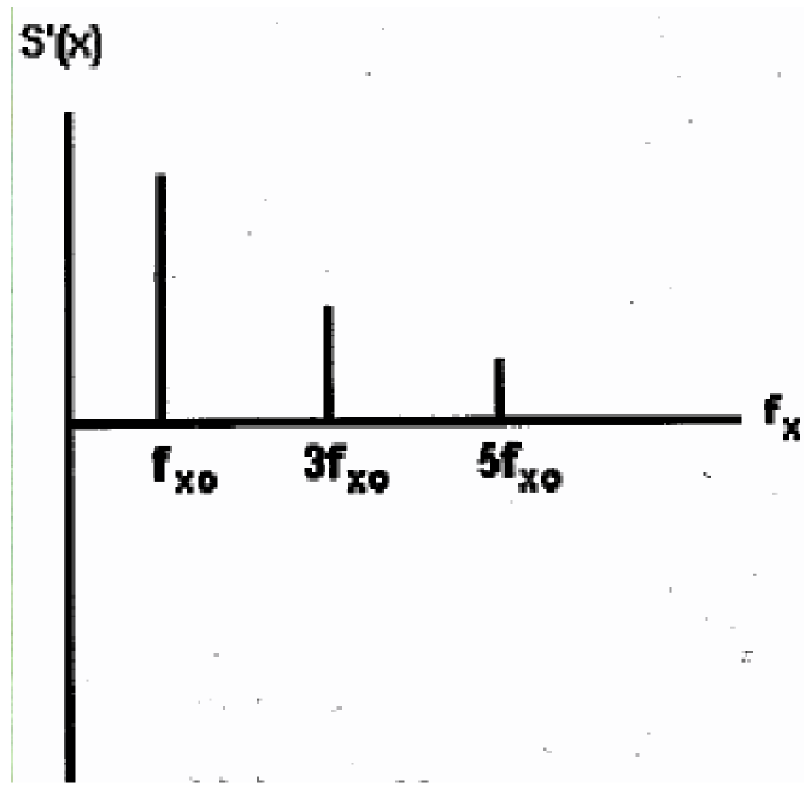

© 1992–2008 R. C. Gonzalez & R. E. Woods

Spatial and Frequency

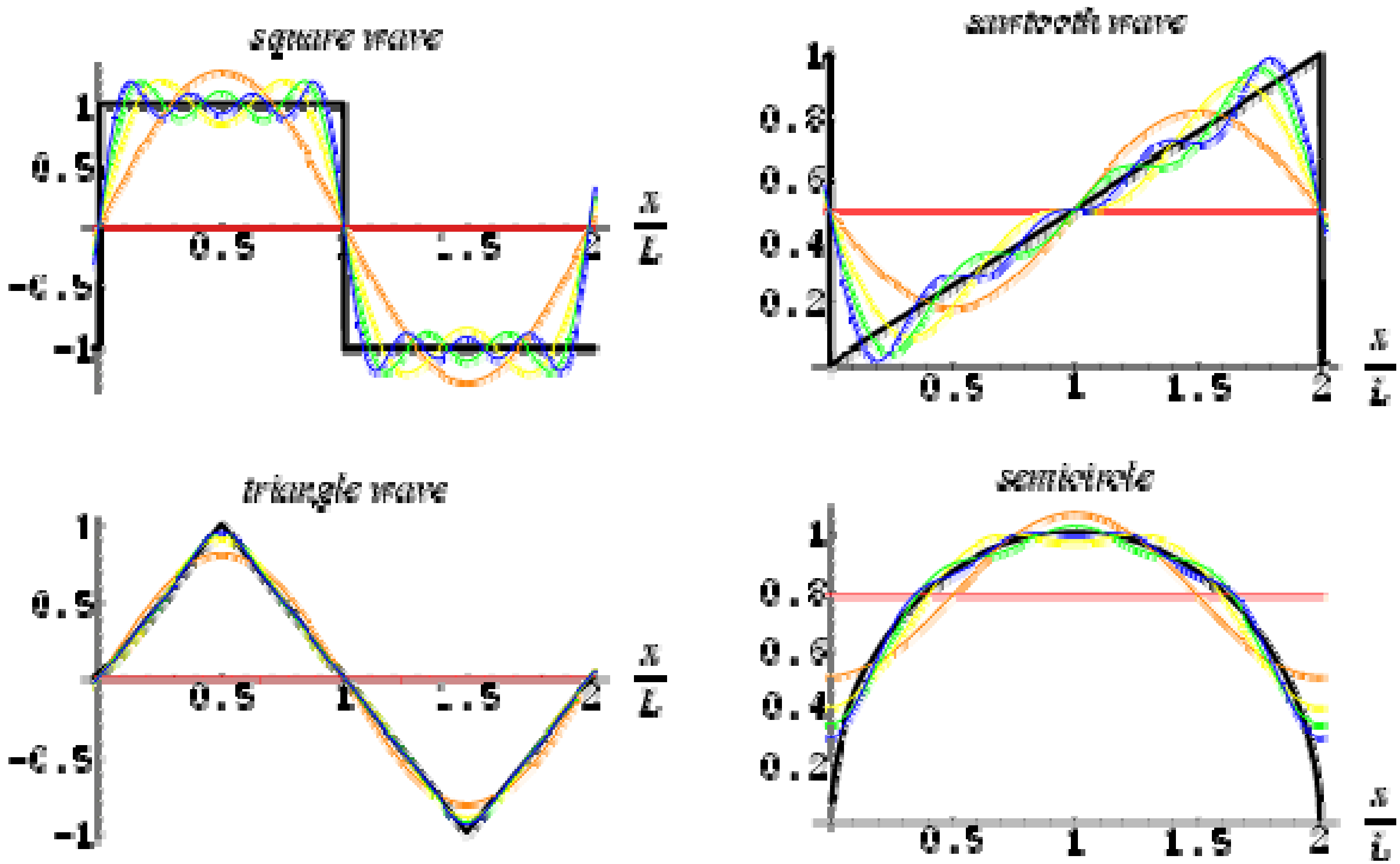

© 1992–2008 R. C. Gonzalez & R. E. Woods

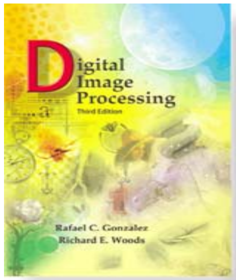

Spatial and Frequency Representations

Spatial Domain

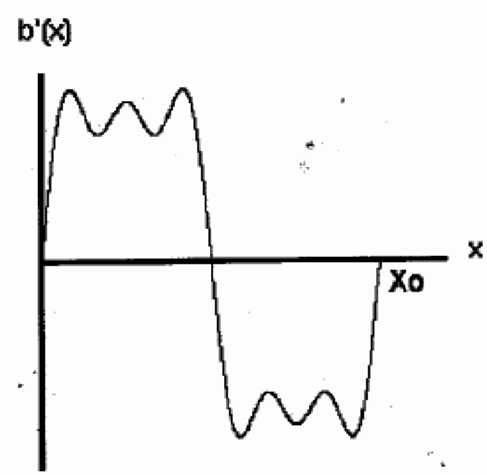

Frequency Domain

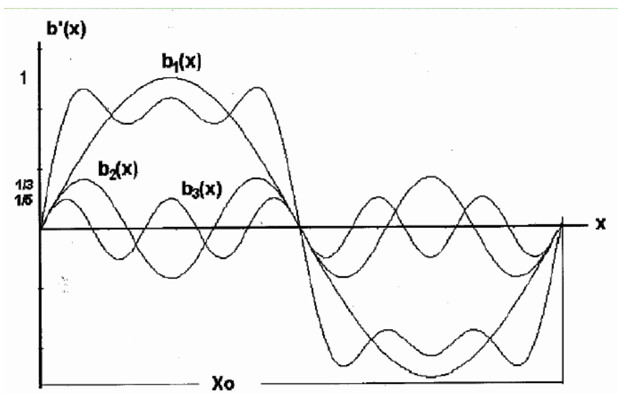

$$b'(x) = b_1(x) + b_2(x) + b_3(x)$$

$$= \sum_{n=1}^{3} \frac{1}{2n-1} \sin(2\pi(2n-1) f_0 x$$

$$b_1(x) = \sin(2\pi f_0 X)$$

$$b_2(x) = \frac{1}{3} \sin(2\pi 3 f_0 X)$$

$$b_3(x) = \frac{1}{5} \sin(2\pi 5 f_0 X)$$

© 1992–2008 R. C. Gonzalez & R. E. Woods

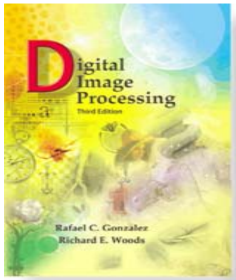

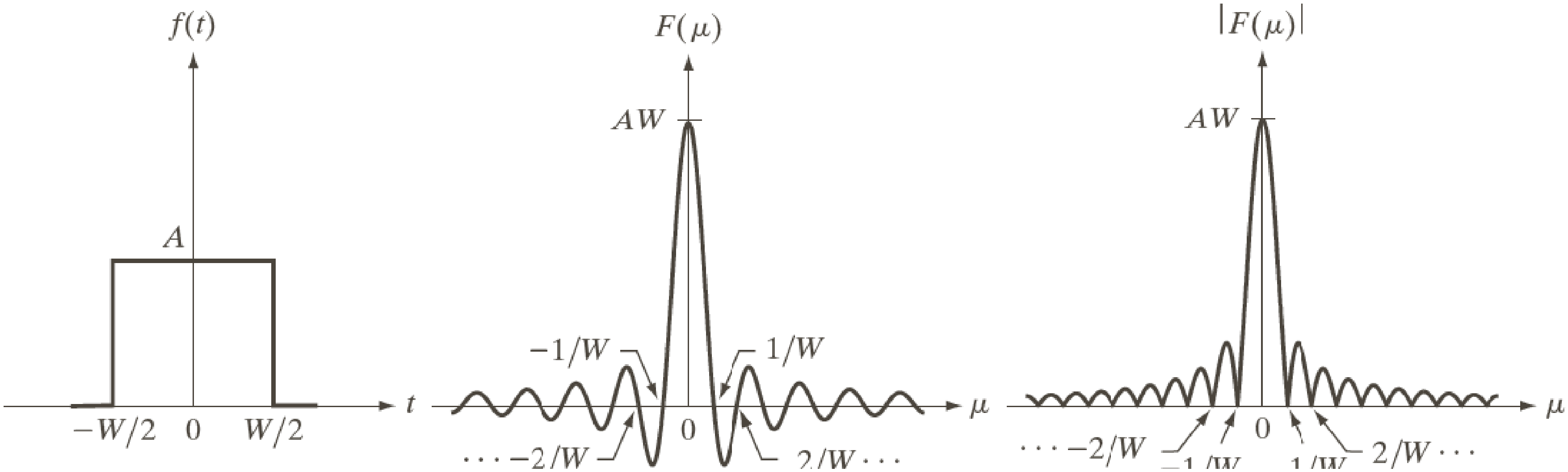

$$F(u)=\int_{-\infty}^{\infty} f(t)e^{-j2\pi ut}dt=\int_{-W/2}^{W/2} Ae^{-j2\pi ut}dt=\frac{-A}{j2\pi u}\left[e^{-j2\pi ut}\right]_{-W/2}^{W/2}$$

$$=$$

© 1992–2008 R. C. Gonzalez & R. E. Woods

2D Fourier Transform

For a give function *g(x)* of a real variable x, the Fourier transformation of *g(x)* which is denoted as

$$\Im\{g(x,y)\} = G(u,v) = \int_{-\infty}^{\infty}\int g(x,y)e^{-j2\pi(ux+vy)}dxdy$$

and

$$\Im^{-1}\{G(u,v)\} = g(x,y) = \int_{-\infty}^{\infty}\int G(u,v)e^{j2\pi(ux+vy)}dudv$$

© 1992–2008 R. C. Gonzalez & R. E. Woods

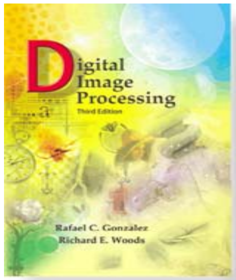

Chapter 4

Filtering in the Frequency Domain

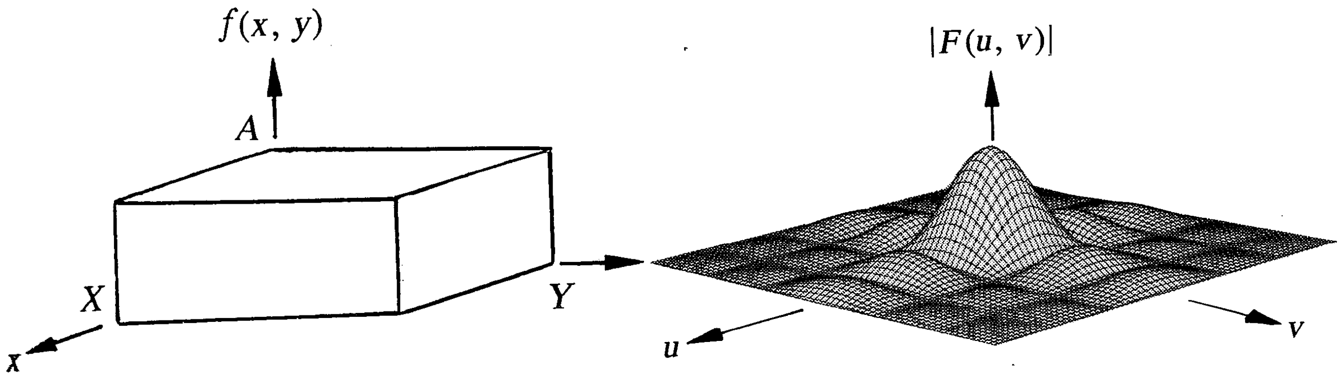

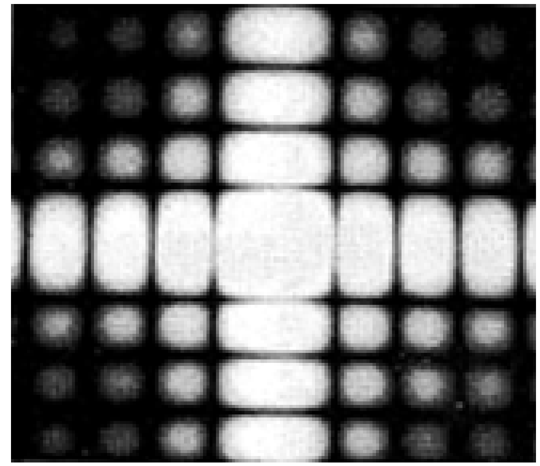

$$F(u,v)=\int_{-\infty}^{\infty}\int_{-\infty}^{\infty} f(x,y)e^{-j2\pi(ux\_vy)}dxdy = A\int_0^X e^{-j2\pi(ux)}dx\int_0^Y e^{-j2\pi(uy)}dy$$

$$= A\left[\frac{e^{-j2\pi(ux)}}{-j2\pi u}\right]_0^X\left[\frac{e^{-j2\pi(vy)}}{-j2\pi v}\right]_0^Y = \frac{A}{-j2\pi u}[e^{-j2\pi(uX)}-1]\frac{A}{-j2\pi v}[e^{-j2\pi(vY)}-1]$$

$$= AXY\left[\frac{\sin(\pi uX)}{\pi uX}\right]\left[\frac{\sin(\pi vY)}{\pi vY}\right]$$

© 1992–2008 R. C. Gonzalez & R. E. Woods

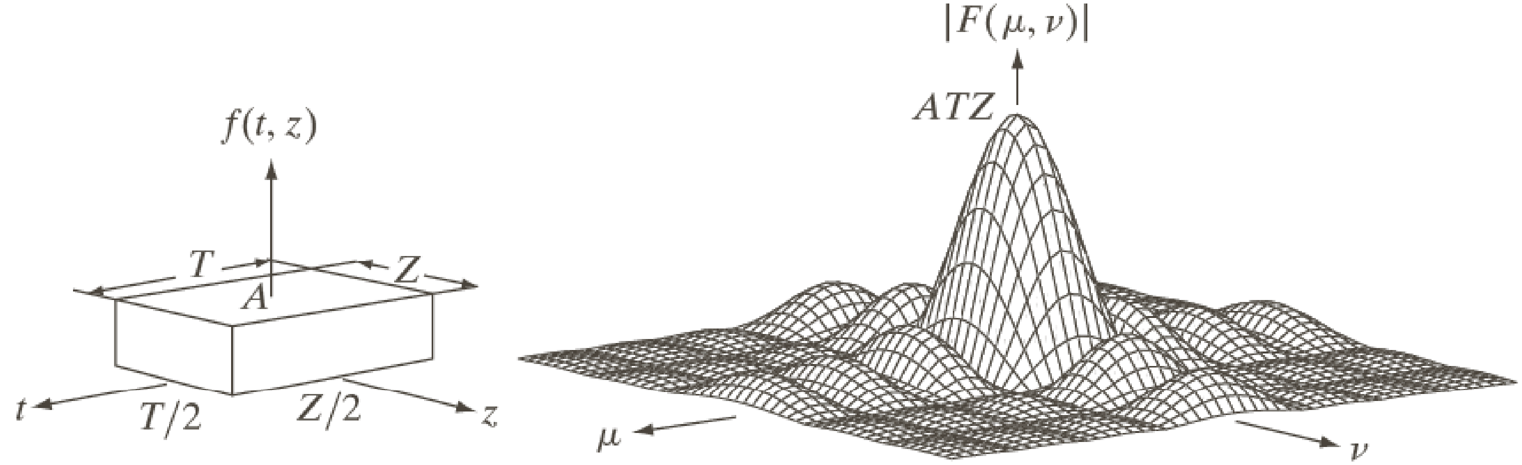

a b

FIGURE 4.13 (a) A 2-D function, and (b) a section of its spectrum (not to scale). The block is longer along the t-axis, so the spectrum is more "contracted" along the μ-axis. Compare with Fig. 4.4.

© 1992–2008 R. C. Gonzalez & R. E. Woods

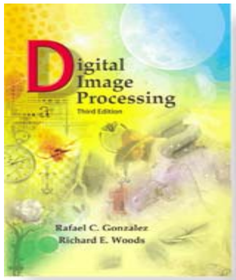

Discrete Fourier Transform

- Let us discretize a continuous function f(x) into the N uniform samples that generate the sequence
  $f(x_0), f(x_0+\Delta x), f(x_0+2\Delta x), f(x_0+3\Delta x), \ldots, f(x_0+[N-1]\Delta x)$
- Hence $f(x) = f(x_0+i\,\Delta x)$
- We could denote the samples as
  f(0), f(1), f(2), …,f(N-1).
- The Fourier Transform is

$$F(u) = \frac{1}{N}\sum_{x=0}^{N-1} f(x)e^{-j2\pi ux/N}; u = 0,1,2,\ldots, N-1$$

and

$$f(x) = \sum_{u=0}^{N-1} F(u)e^{j2\pi ux/N}$$

© 1992–2008 R. C. Gonzalez & R. E. Woods

2D Discrete Fourier Transform

$$F(u,v) = \frac{1}{NM}\sum_{x=0}^{M-1}\sum_{y=0}^{N-1} f(x,y)e^{-j2\pi(ux/M+vy/N)}$$

$$u = 0,1,2,\ldots,M-1; v = 0,1,2,\ldots,N-1$$

and

$$f(x,y) = \sum_{u=0}^{M-1}\sum_{v=0}^{N-1} F(u,v)e^{j2\pi(ux/M+vy/N)}$$

$$\Delta u = \frac{1}{M\Delta x}; \Delta v = \frac{1}{N\Delta y}$$

© 1992–2008 R. C. Gonzalez & R. E. Woods

Display F(u,v)

The Dynamic rang of Fourier spectra usually is much higher than the typical display device is able to reproduce fathfuly. Therefore, often use the logarithm function to perform the appropriate compression of the rang.

$$D(u,v) = c\log(1 + |F(u,v)|)$$

Where c is a scale factor

© 1992–2008 R. C. Gonzalez & R. E. Woods

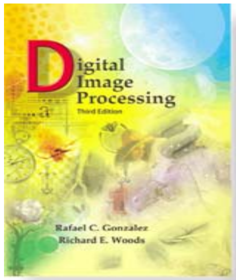

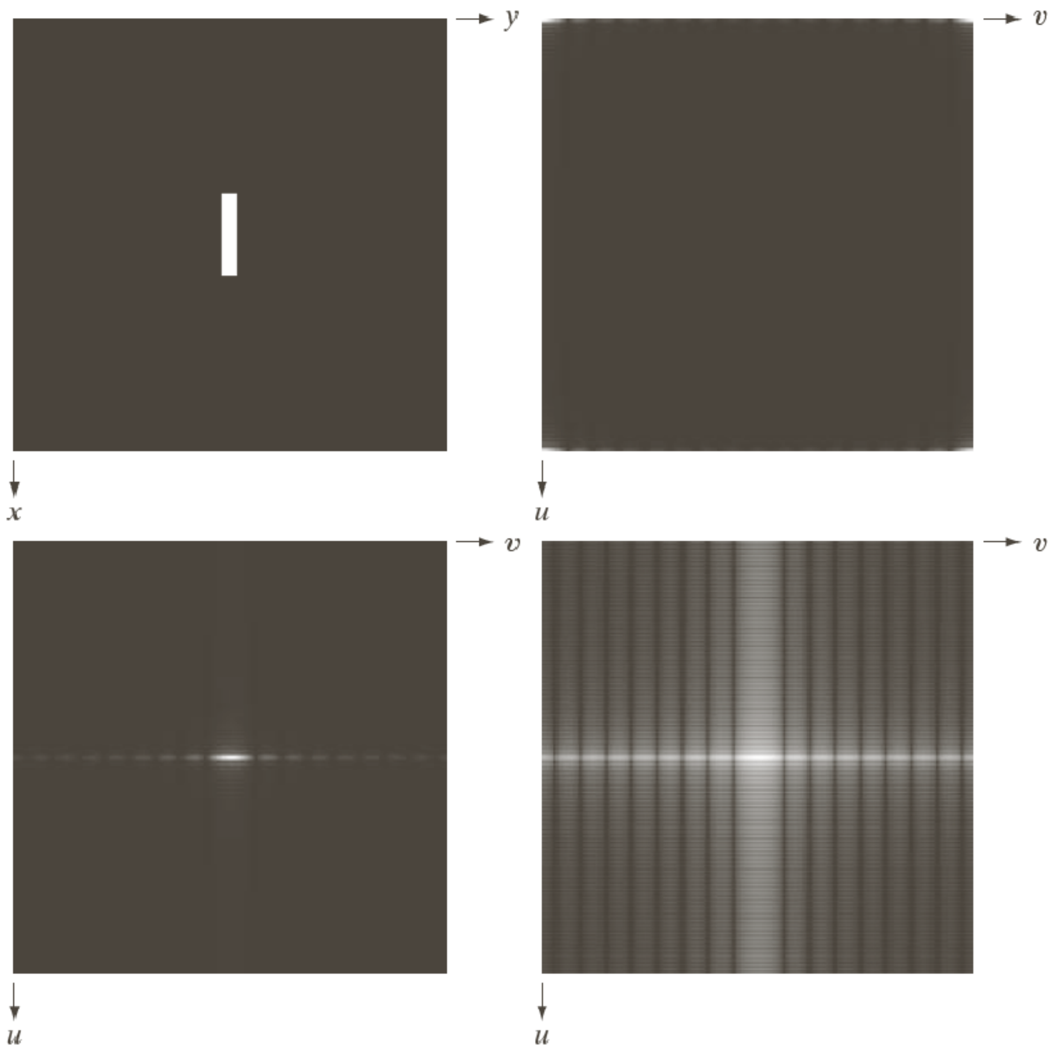

a b
c d

FIGURE 4.24 (a) Image. (b) Spectrum showing bright spots in the four corners. (c) Centered spectrum. (d) Result showing increased detail after a log transformation. The zero crossings of the spectrum are closer in the vertical direction because the rectangle in (a) is longer in that direction. The coordinate convention used throughout the book places the origin of the spatial and frequency domains at the top left.

© 1992–2008 R. C. Gonzalez & R. E. Woods

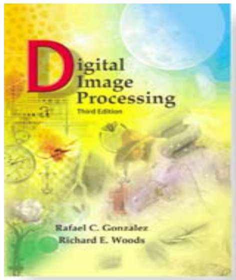

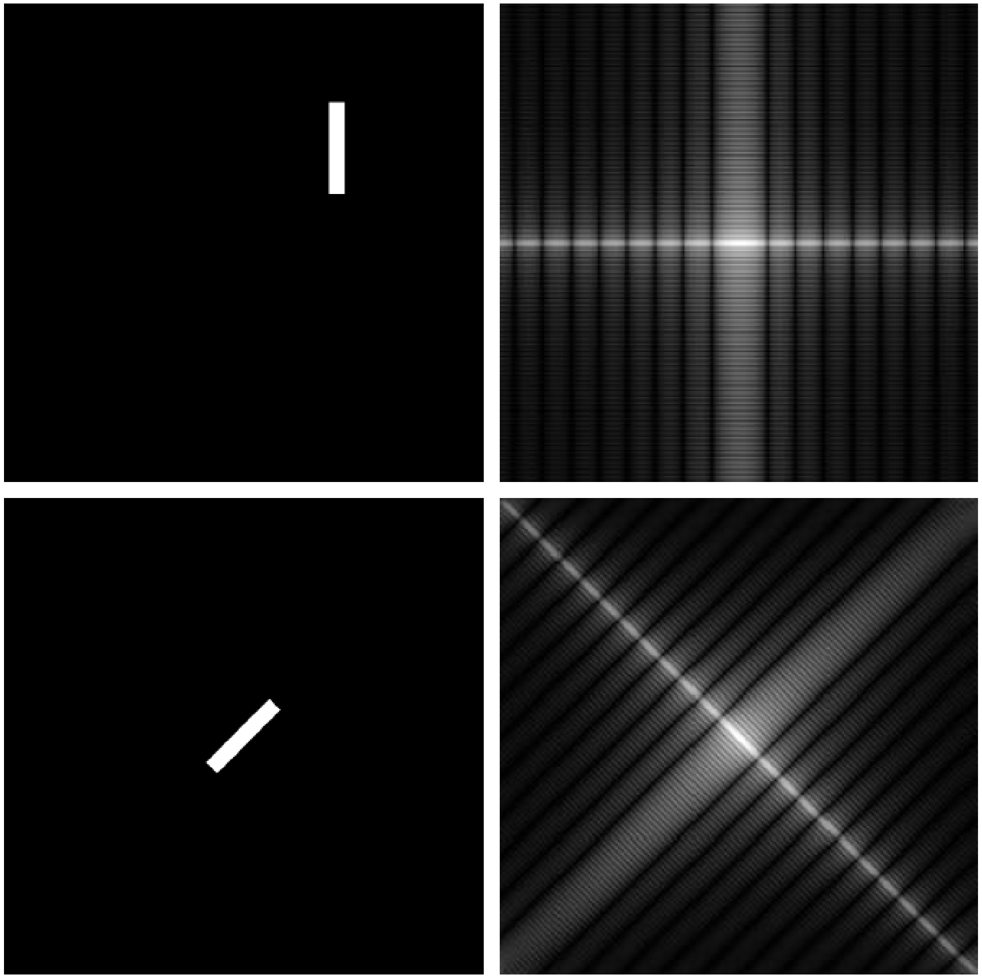

a b
c d

FIGURE 4.25 (a) The rectangle in Fig. 4.24(a) translated, and (b) the corresponding spectrum. (c) Rotated rectangle, and (d) the corresponding spectrum. The spectrum corresponding to the translated rectangle is identical to the spectrum corresponding to the original image in Fig. 4.24(a).

© 1992–2008 R. C. Gonzalez & R. E. Woods

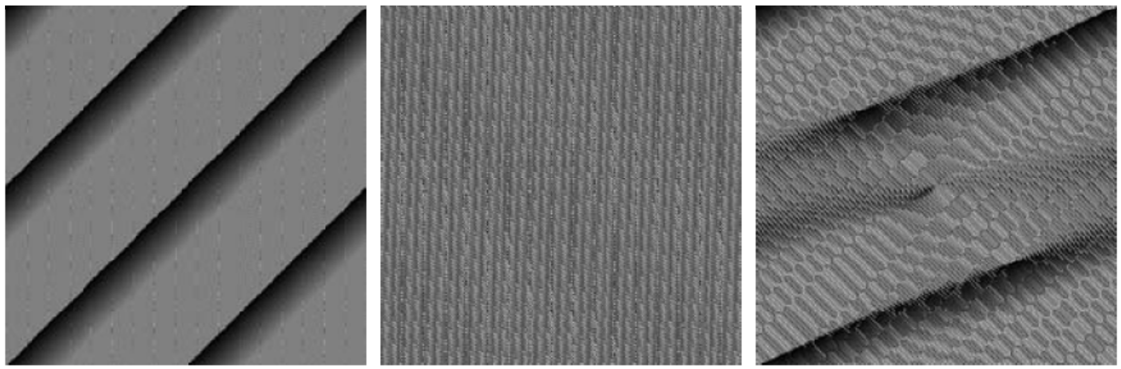

a b c

FIGURE 4.26 Phase angle array corresponding (a) to the image of the centered rectangle in Fig. 4.24(a), (b) to the translated image in Fig. 4.25(a), and (c) to the rotated image in Fig. 4.25(c).

© 1992–2008 R. C. Gonzalez & R. E. Woods

Examples

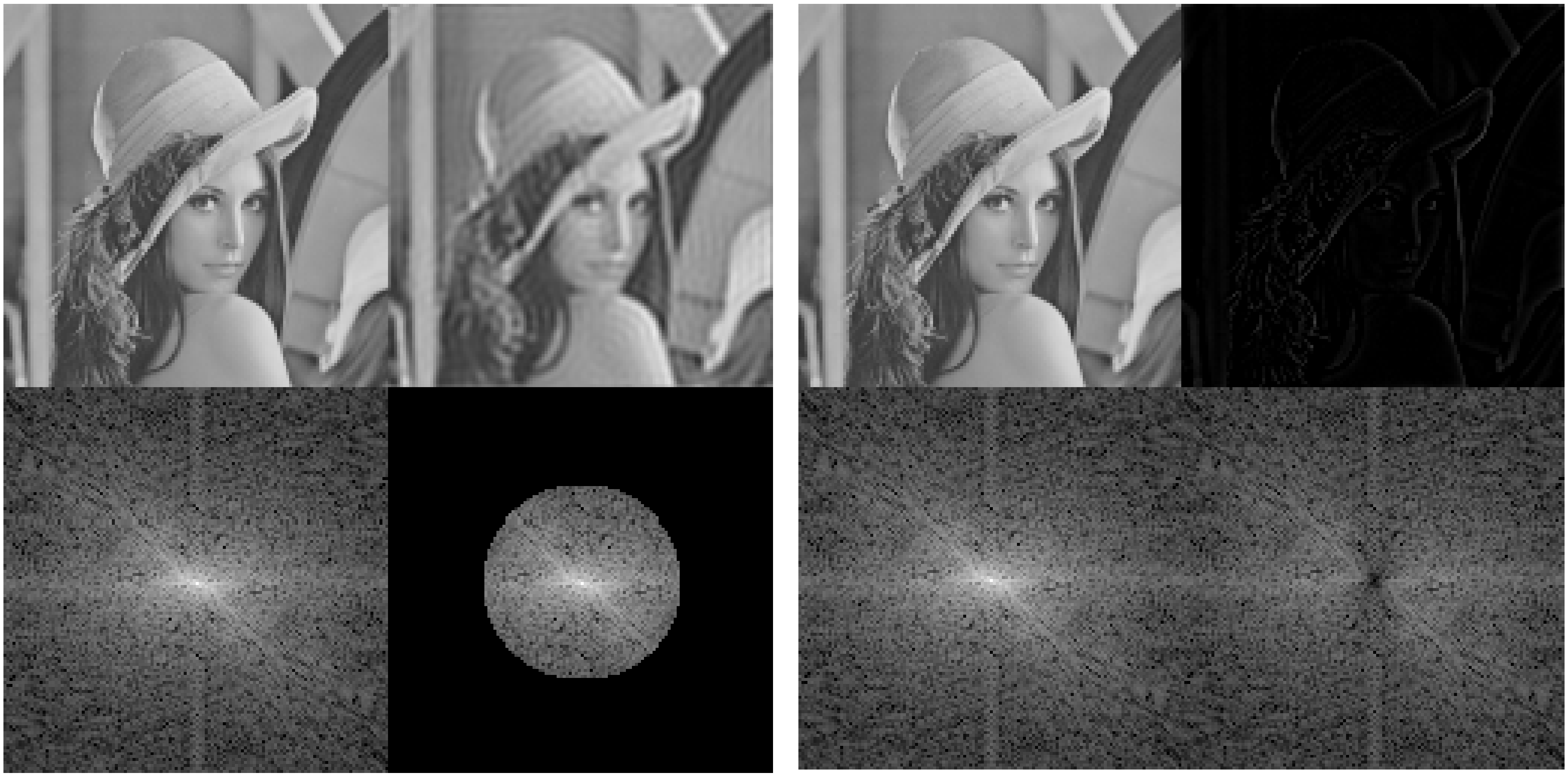

http://www.cs.unm.edu/~brayer/vision/fourier.html

© 1992–2008 R. C. Gonzalez & R. E. Woods

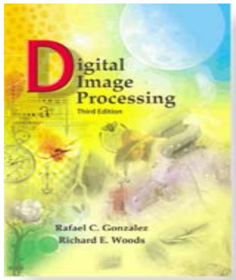

Properties of 2D Fourier Transform

- Spatial and Frequency Domain

f(t, z) sampled from f(x, y) using the separation between samples as ΔT and ΔZ

$$\Delta u = \frac{1}{M\Delta T}$$

$$\Delta v = \frac{1}{N\Delta Z}$$

- Translation and Rotation

Multiplying f(x,y) by the exponential shifts the original of DFT to (u_0,v_0).

Multiplying F(u,v) by the exponential shifts the original of f(x, y) to (x_0,y_0);

$$f(x-x_0, y-y_0) \Leftrightarrow F(u,v)e^{j2\pi(x_0 u/M + y_0 v/N)}$$

$$F(u-u_0, v-v_0) \Leftrightarrow f(x,y)e^{-j2\pi(u_0 x/M + v_0 y/N)}$$

© 1992–2008 R. C. Gonzalez & R. E. Woods

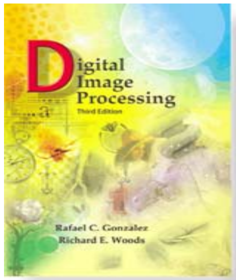

Properties of 2D Fourier Transform

Periodicity

The Fourier transform and inverse are infinitely periodic on the u and v directions. (k_1 and k_2 are integers).

$$F(u,v) = F(u+k_1M, v) = F(u, v+k_2N)$$
$$= F(u+k_1M, v+k_2N)$$
$$f(x,y) = f(x+k_1M, y) = f(x, y+k_2N)$$
$$= f(x+k_1M, y+k_2N)$$

To show the origin of F(u,v) at the center we shift the data by M/2 and N/2

$$f(x,y)(-1)^{x+y} = F(u+M/2, v+N/2)$$

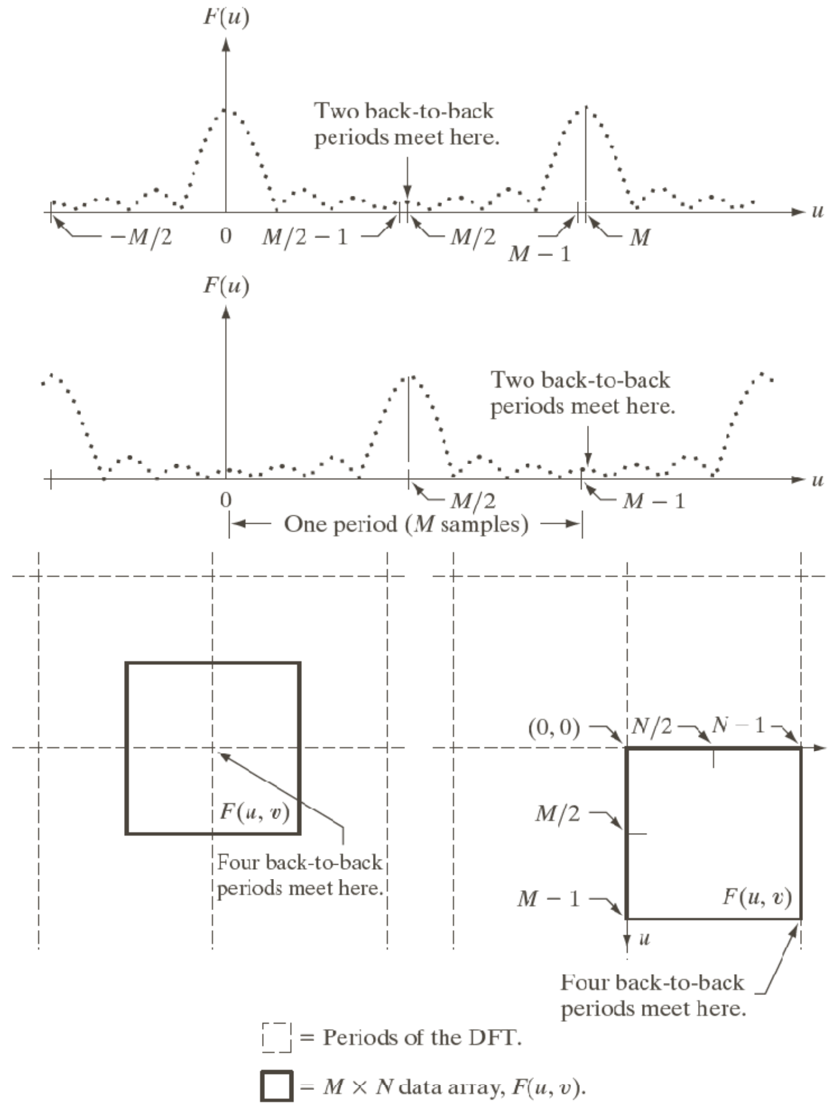

© 1992–2008 R. C. Gonzalez & R. E. Woods

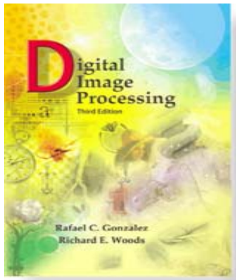

Properties of 2D Fourier Transform

Symmetry

Any real or complex function can be expressed as the sum of even and odd part

$$w(x,y) = w_e(x,y) + w_o(x,y)$$

$$w_e(x,y) \stackrel{\Delta}{=} \frac{w(x,y) + w(-x,-y)}{2}$$

$$w_e(x,y) \stackrel{\Delta}{=} \frac{w(x,y) - w(-x,-y)}{2}$$

Which shows that even functions are symmetric and odd functions are antisymmetric

$$w_e(x,y) = w_e(-x,-y)$$

$$w_o(x,y) = -w_o(-x,-y)$$

© 1992–2008 R. C. Gonzalez & R. E. Woods

Properties of 2D Fourier Transform

Symmetry

The Fourier transform of a real function f(x,y) is conjugate symmetric

$$F^*(u,v) = F(-u,-v)$$

The Fourier transform of a imaginary function f(x,y) is conjugate anti-symmetric

$$F^*(-u,-v) = -F(u,v)$$

Proof

$$F^*(u,v) = \left[\frac{1}{NM} \sum_{x=0}^{M-1} \sum_{y=0}^{N-1} f(x,y) e^{-j2\pi(ux/M + vy/N)} \right]^*$$

$$= \frac{1}{NM} \sum_{x=0}^{M-1} \sum_{y=0}^{N-1} f^*(x,y) e^{j2\pi(ux/M + vy/N)}$$

$$= \frac{1}{NM} \sum_{x=0}^{M-1} \sum_{y=0}^{N-1} f(x,y) e^{-j2\pi([-u]x/M + [-v]y/N)}$$

$$= F(-u,-v)$$

© 1992–2008 R. C. Gonzalez & R. E. Woods

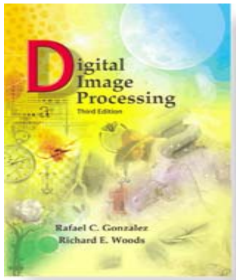

Chapter 4
Filtering in the Frequency Domain

	Spatial Domain†		Frequency Domain†
1)	$f(x, y)$ real	$\Leftrightarrow$	$F^*(u, v) = F(-u, -v)$
2)	$f(x, y)$ imaginary	$\Leftrightarrow$	$F^*(-u, -v) = -F(u, v)$
3)	$f(x, y)$ real	$\Leftrightarrow$	$R(u, v)$ even; $I(u, v)$ odd
4)	$f(x, y)$ imaginary	$\Leftrightarrow$	$R(u, v)$ odd; $I(u, v)$ even
5)	$f(-x, -y)$ real	$\Leftrightarrow$	$F^*(u, v)$ complex
6)	$f(-x, -y)$ complex	$\Leftrightarrow$	$F(-u, -v)$ complex
7)	$f^*(x, y)$ complex	$\Leftrightarrow$	$F^*(-u - v)$ complex
8)	$f(x, y)$ real and even	$\Leftrightarrow$	$F(u, v)$ real and even
9)	$f(x, y)$ real and odd	$\Leftrightarrow$	$F(u, v)$ imaginary and odd
10)	$f(x, y)$ imaginary and even	$\Leftrightarrow$	$F(u, v)$ imaginary and even
11)	$f(x, y)$ imaginary and odd	$\Leftrightarrow$	$F(u, v)$ real and odd
12)	$f(x, y)$ complex and even	$\Leftrightarrow$	$F(u, v)$ complex and even
13)	$f(x, y)$ complex and odd	$\Leftrightarrow$	$F(u, v)$ complex and odd

© 1992–2008 R. C. Gonzalez & R. E. Woods

Convolution

$$f(x,y) \bigstar h(x,y) = \sum_{m=0}^{M-1}\sum_{n=0}^{N-1} f(m,n)h(x-m,y-n)$$

Correlation

$$f(x,y) \star h(x,y) = \sum_{m=0}^{M-1}\sum_{n=0}^{N-1} f^{*}(m,n)h(x+m,y+n)$$

© 1992–2008 R. C. Gonzalez & R. E. Woods

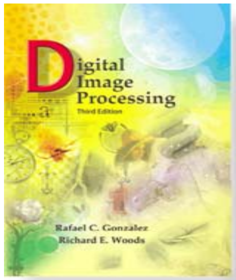

Name	DFT Pairs
Correlation theorem†	$f(x,y) \star h(x,y) \Leftrightarrow F^*(u,v)\,H(u,v)$ $f^*(x,y)h(x,y) \Leftrightarrow F(u,v) \star H(u,v)$
Discrete unit impulse	$\delta(x,y) \Leftrightarrow 1$
Rectangle	$\text{rect}[a,b] \Leftrightarrow ab\dfrac{\sin(\pi ua)}{(\pi ua)}\dfrac{\sin(\pi vb)}{(\pi vb)}e^{-j\pi(ua+vb)}$
Sine	$\sin(2\pi u_0 x + 2\pi v_0 y) \Leftrightarrow$ $j\dfrac{1}{2}\left[\delta(u + Mu_0, v + Nv_0) - \delta(u - Mu_0, v - Nv_0)\right]$
Cosine	$\cos(2\pi u_0 x + 2\pi v_0 y) \Leftrightarrow$ $\dfrac{1}{2}\left[\delta(u + Mu_0, v + Nv_0) + \delta(u - Mu_0, v - Nv_0)\right]$

© 1992–2008 R. C. Gonzalez & R. E. Woods

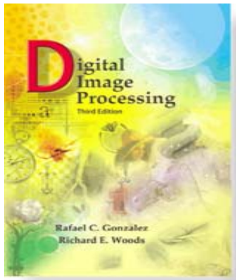

Name	Expression(s)
1) Discrete Fourier transform (DFT) of $f(x, y)$	$F(u, v) = \sum_{x=0}^{M-1} \sum_{y=0}^{N-1} f(x, y)\, e^{-j2\pi(ux/M + vy/N)}$
2) Inverse discrete Fourier transform (IDFT) of $F(u, v)$	$f(x, y) = \frac{1}{MN} \sum_{u=0}^{M-1} \sum_{v=0}^{N-1} F(u, v)\, e^{j2\pi(ux/M + vy/N)}$
3) Polar representation	$F(u, v) = \lvert F(u, v) \rvert e^{j\phi(u,v)}$
4) Spectrum	$\lvert F(u, v) \rvert = \left[R^2(u, v) + I^2(u, v) \right]^{1/2}$ $R = \text{Real}(F); \quad I = \text{Imag}(F)$
5) Phase angle	$\phi(u, v) = \tan^{-1}\left[\frac{I(u, v)}{R(u, v)} \right]$
6) Power spectrum	$P(u, v) = \lvert F(u, v) \rvert^2$
7) Average value	$\bar{f}(x, y) = \frac{1}{MN} \sum_{x=0}^{M-1} \sum_{y=0}^{N-1} f(x, y) = \frac{1}{MN} F(0, 0)$

(*Coninued*)

© 1992–2008 R. C. Gor

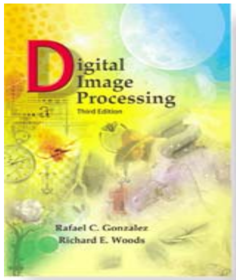

Chapter 4
Filtering in the Frequency Domain

Name	Expression(s)
8) Periodicity (k_1 and k_2 are integers)	$F(u,v) = F(u + k_1M, v) = F(u, v + k_2N) = F(u + k_1M, v + k_2N)$ $f(x,y) = f(x + k_1M, y) = f(x, y + k_2N) = f(x + k_1M, y + k_2N)$
9) Convolution	$f(x,y) \bigstar h(x,y) = \sum_{m=0}^{M-1}\sum_{n=0}^{N-1} f(m,n)h(x-m, y-n)$
10) Correlation	$f(x,y) \star h(x,y) = \sum_{m=0}^{M-1}\sum_{n=0}^{N-1} f^*(m,n)h(x+m, y+n)$
11) Separability	The 2-D DFT can be computed by computing 1-D DFT transforms along the rows (columns) of the image, followed by 1-D transforms along the columns (rows) of the result. See Section 4.11.1.
12) Obtaining the inverse Fourier transform using a forward transform algorithm.	$MNf^*(x,y) = \sum_{u=0}^{M-1}\sum_{v=0}^{N-1} F^*(u,v)e^{-j2\pi(ux/M + vy/N)}$ This equation indicates that inputting $F^*(u,v)$ into an algorithm that computes the forward transform (right side of above equation) yields $MNf^*(x,y)$. Taking the complex conjugate and dividing by MN gives the desired inverse. See Section 4.11.2.

© 1992–2008 R. C. Gonzalez & R. E. Woods

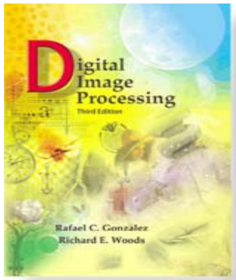

Chapter 4
Filtering in the Frequency Domain

Name	DFT Pairs
1) Symmetry properties	See Table 4.1
2) Linearity	$af_1(x, y) + bf_2(x, y) \Leftrightarrow aF_1(u, v) + bF_2(u, v)$
3) Translation (general)	$f(x, y)e^{j2\pi(u_0x/M - v_0y/N)} \Leftrightarrow F(u - u_0, v - v_0)$ $f(x - x_0, y - y_0) \Leftrightarrow F(u, v)e^{-j2\pi(ux_0/M + vy_0/N)}$
4) Translation to center of the frequency rectangle, $(M/2, N/2)$	$f(x, y)(-1)^{x+y} \Leftrightarrow F(u - M/2, v - N/2)$ $f(x - M/2, y - N/2) \Leftrightarrow F(u, v)(-1)^{u+v}$
5) Rotation	$f(r, \theta + \theta_0) \Leftrightarrow F(\omega, \varphi + \theta_0)$ $x = r\cos\theta \quad y = r\sin\theta \quad u = \omega\cos\varphi \quad v = \omega\sin\varphi$
6) Convolution theorem†	$f(x, y) \star h(x, y) \Leftrightarrow F(u, v)H(u, v)$ $f(x, y)h(x, y) \Leftrightarrow F(u, v) \star H(u, v)$

(Continued)

© 1992–2008 R. C. Gonzalez & R. E. Woods

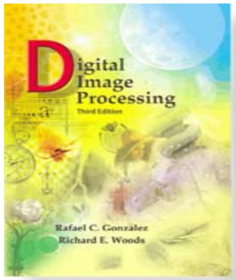

Chapter 4
Filtering in the Frequency Domain

	Name	DFT Pairs
7)	Correlation theorem†	$f(x, y) \star h(x, y) \Leftrightarrow F^*(u, v)\, H(u, v)$ $f^*(x, y) h(x, y) \Leftrightarrow F(u, v) \star H(u, v)$
8)	Discrete unit impulse	$\delta(x, y) \Leftrightarrow 1$
9)	Rectangle	$\text{rect}[a, b] \Leftrightarrow ab \dfrac{\sin(\pi ua)}{(\pi ua)} \dfrac{\sin(\pi vb)}{(\pi vb)} e^{-j\pi(ua+vb)}$
10)	Sine	$\sin(2\pi u_0 x + 2\pi v_0 y) \Leftrightarrow$ $j\frac{1}{2}\left[\delta(u + Mu_0, v + Nv_0) - \delta(u - Mu_0, v - Nv_0)\right]$
11)	Cosine	$\cos(2\pi u_0 x + 2\pi v_0 y) \Leftrightarrow$ $\frac{1}{2}\left[\delta(u + Mu_0, v + Nv_0) + \delta(u - Mu_0, v - Nv_0)\right]$
	The following Fourier transform pairs are derivable only for continuous variables, denoted as before by t and z for spatial variables and by μ and ν for frequency variables. These results can be used for DFT work by sampling the continuous forms.	
12)	*Differentiation* (The expressions on the right assume that $f(\pm\infty, \pm\infty) = 0$.)	$\left(\frac{\partial}{\partial t}\right)^m \left(\frac{\partial}{\partial z}\right)^n f(t, z) \Leftrightarrow (j2\pi\mu)^m (j2\pi\nu)^n F(\mu, \nu)$ $\dfrac{\partial^m f(t, z)}{\partial t^m} \Leftrightarrow (j2\pi\mu)^m F(\mu, \nu); \dfrac{\partial^n f(t, z)}{\partial z^n} \Leftrightarrow (j2\pi\nu)^n F(\mu, \nu)$
13)	*Gaussian*	$A2\pi\sigma^2 e^{-2\pi^2\sigma^2(t^2+z^2)} \Leftrightarrow Ae^{-(\mu^2+\nu^2)/2\sigma^2}$ (A is a constant)

†Assumes that the functions have been extended by zero padding. Convolution and correlation are associative, commutative, and distributive.

© 1992–2008 R. C. Gonzalez & R. E. Woods

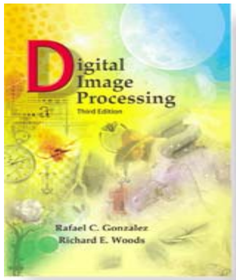

Sampling and Fourier Transform

1. Converting continuous function/signal into a discrete one.
2. The sampling is uniform at ΔT intervals

The sampled function and the value of each Sample are :

$$\tilde{f}(t) = f(t)s_{\Delta T}(t) = \sum_{n=-\infty}^{\infty} f(t)\delta(t - n\Delta T)$$

$$f_k = \int_{-\infty}^{\infty} f(t)\delta(t - k\Delta T)dt = f(k\Delta T)$$

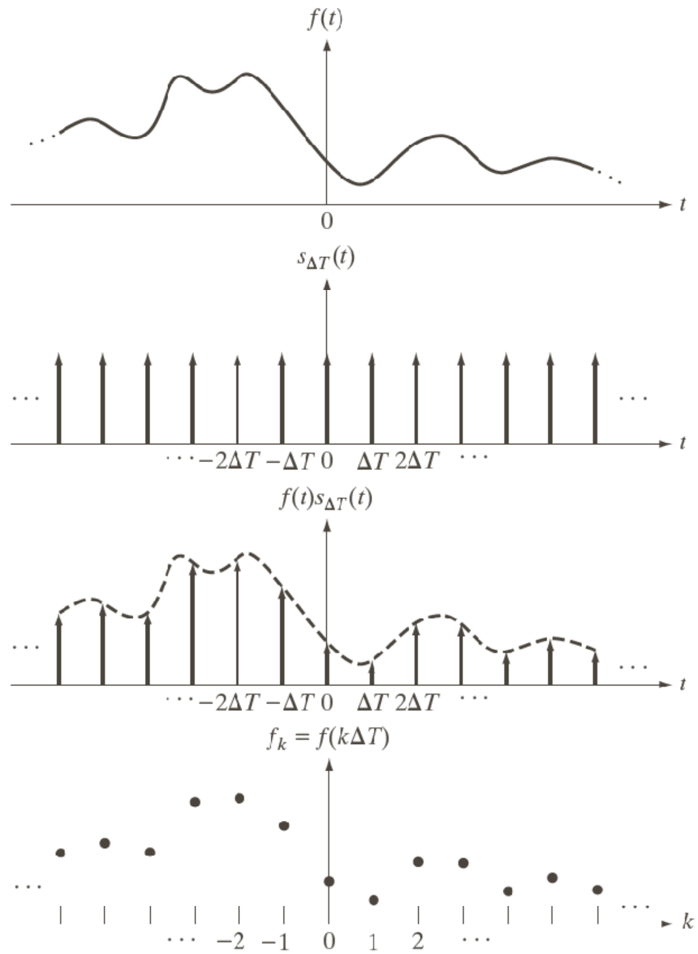

© 1992–2008 R. C. Gonzalez & R. E. Woods

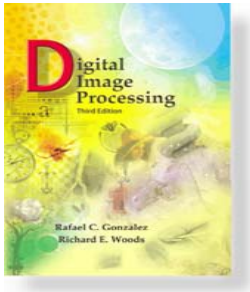

The Fourier of Sampled function

Let F(μ) and $\tilde{F}(\mu)$ be the Fourier transform of the continuous function f(t) and its equivalent Sampled function $\tilde{f}(t)$

$$\tilde{F}(\mu) = \Im\{\tilde{f}(t)\} = \Im\{f(t)s_{\Delta T}(t)\} = F(\mu) \circ S(\mu)$$

$$S(\mu) = \frac{1}{\Delta T}\sum_{n=-\infty}^{\infty}\delta(\mu - \frac{n}{\Delta T})$$

$$\tilde{F}(\mu) = F(\mu) \circ S(\mu) = \int_{-\infty}^{\infty} F(\tau)S(\mu-\tau)d\tau$$

$$= \frac{1}{\Delta T}\int_{-\infty}^{\infty} F(\tau)\sum_{n=-\infty}^{\infty}\delta(\mu - \tau - \frac{n}{\Delta T})d\tau$$

$$= \frac{1}{\Delta T}\sum_{n=-\infty}^{\infty}\int_{-\infty}^{\infty} F(\tau)\delta(\mu - \tau - \frac{n}{\Delta T})d\tau$$

$$= \frac{1}{\Delta T}\sum_{n=-\infty}^{\infty} F\left(\mu - \frac{n}{\Delta T}\right)$$

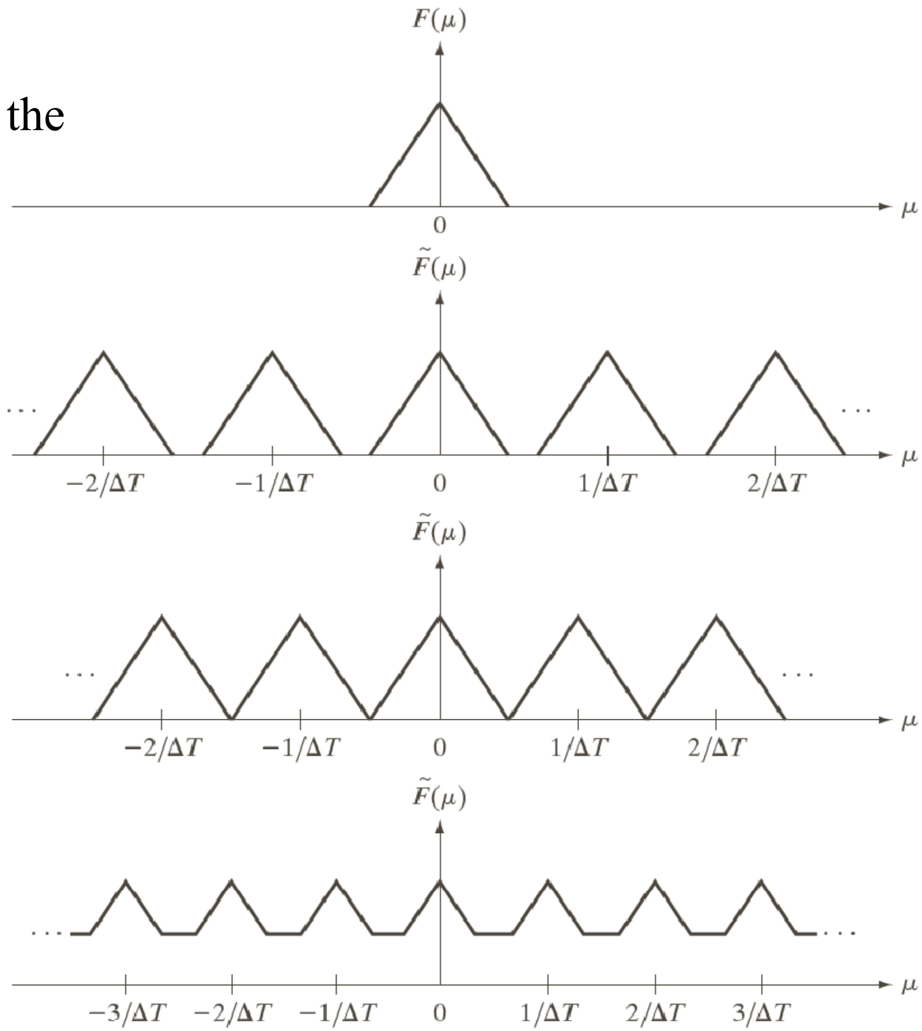

© 1992–2008 R. C. Gonzalez & R. E. Woods

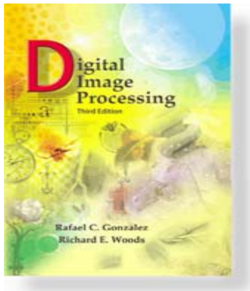

Sampling Theorem

***Band limited*-**A function f(t) whose Fourier transform is zero out of the interval [$-\mu_{max}$, μ_{max}] is called band limited

We can recover a function f(t) from its sampled representation if we can isolate a copy of F(μ) from the periodic sequence of copies.

Extracting from $\tilde{F}(\mu)$ a single period that represents F(μ) is possible in the separation between copies is sufficient , which is guaranteed if $\frac{1}{2\Delta T} > \mu_{max}$

$$\frac{1}{\Delta T} > 2\mu_{\max}$$

Which is call the Nyquist Rate

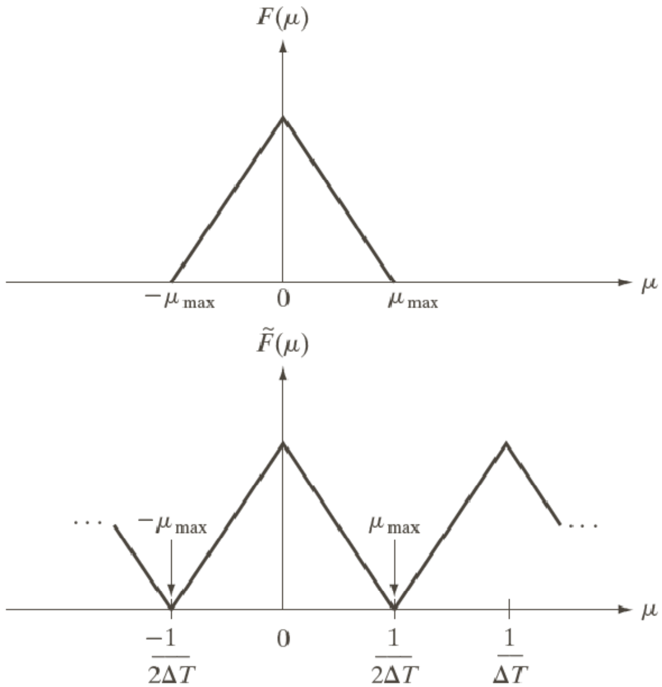

© 1992–2008 R. C. Gonzalez & R. E. Woods

To extract a single copy we multiply $\tilde{F}(\mu)$ by $H(\mu)$.

$$H(\mu) = \begin{cases} \Delta T & -\mu_{\max} \le \mu \le \mu_{\max} \\ 0 & otherwise \end{cases}$$

$$F(\mu) = H(\mu)\tilde{F}(\mu)$$

Once we have $F(\mu)$ we can recover $f(t)$

$$f(t) = \int_{-\infty}^{\infty} F(\mu) e^{j2\pi\mu t} d\mu$$

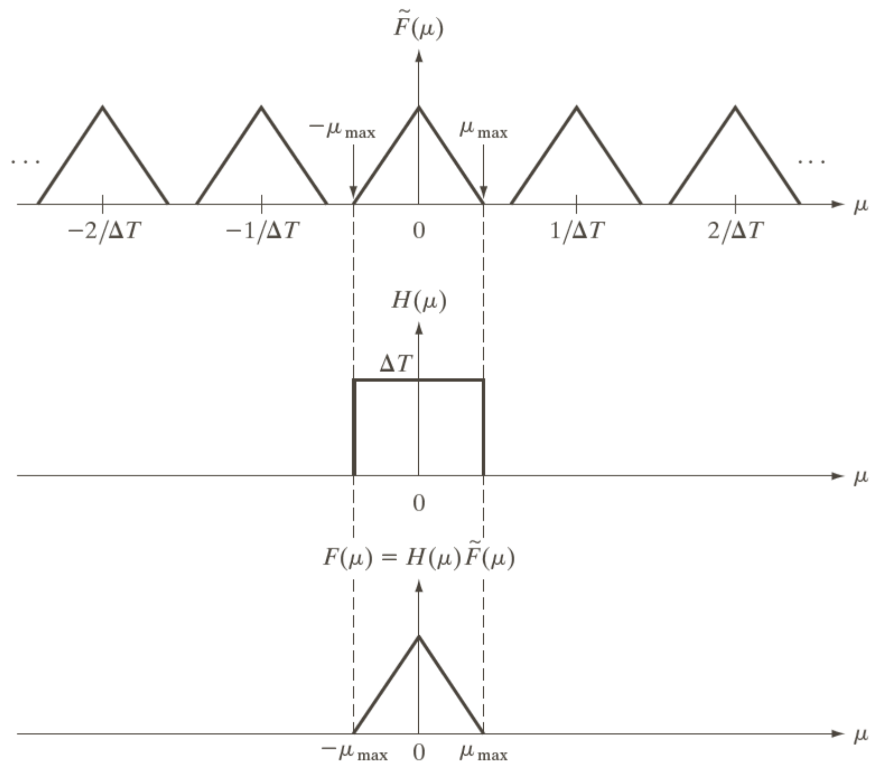

© 1992–2008 R. C. Gonzalez & R. E. Woods

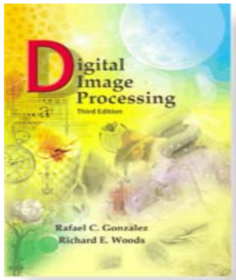

Aliasing

Appears when the sampling rate is less than the Nyquist rate – under-sampling. The inverse Fourier transform would then yield a corrupted function of t, which is known as frequency aliasing or just aliasing.

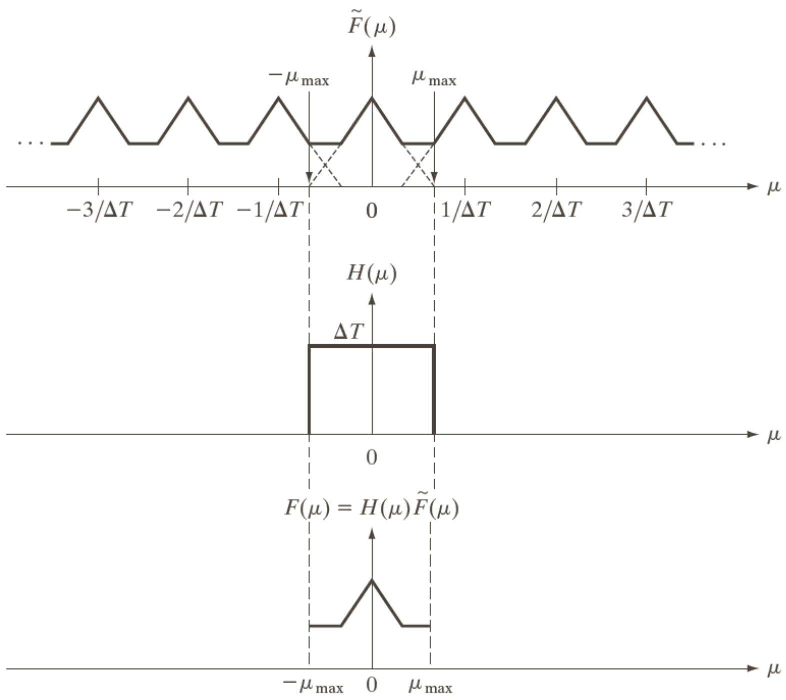

© 1992–2008 R. C. Gonzalez & R. E. Woods

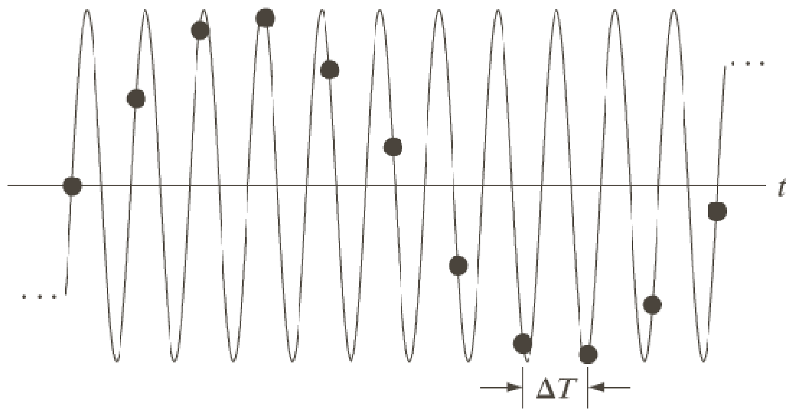

FIGURE 4.10 Illustration of aliasing. The under-sampled function (black dots) looks like a sine wave having a frequency much lower than the frequency of the continuous signal. The period of the sine wave is 2 s, so the zero crossings of the horizontal axis occur every second. ΔT is the separation between samples.

© 1992–2008 R. C. Gonzalez & R. E. Woods

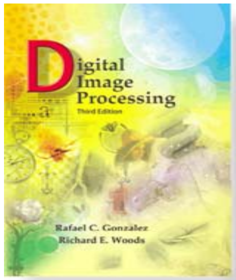

Sampling in the 2D Domain

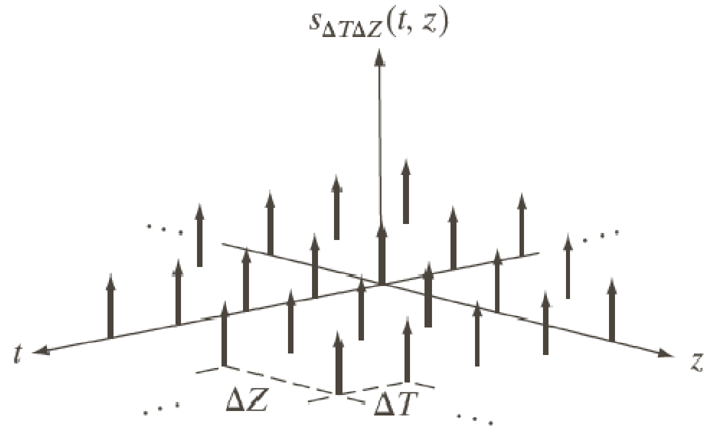

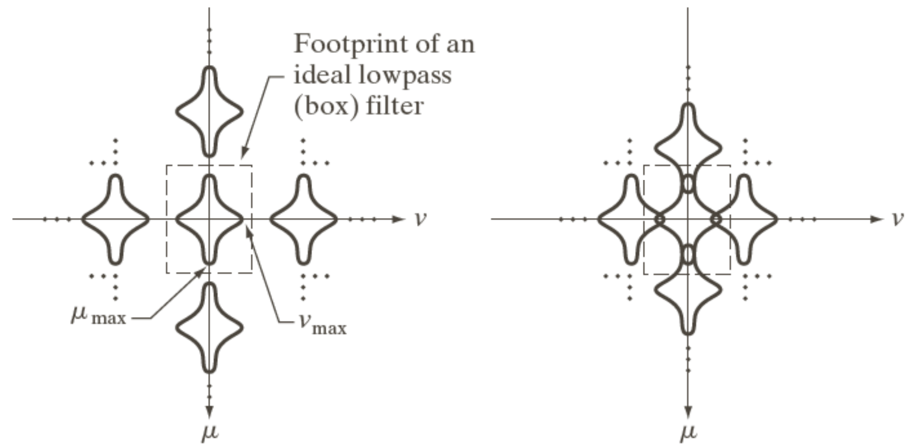

© 1992–2008 R. C. Gonzalez & R. E. Woods

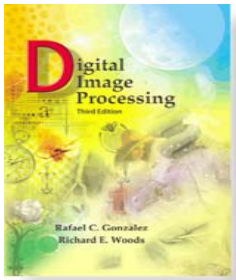

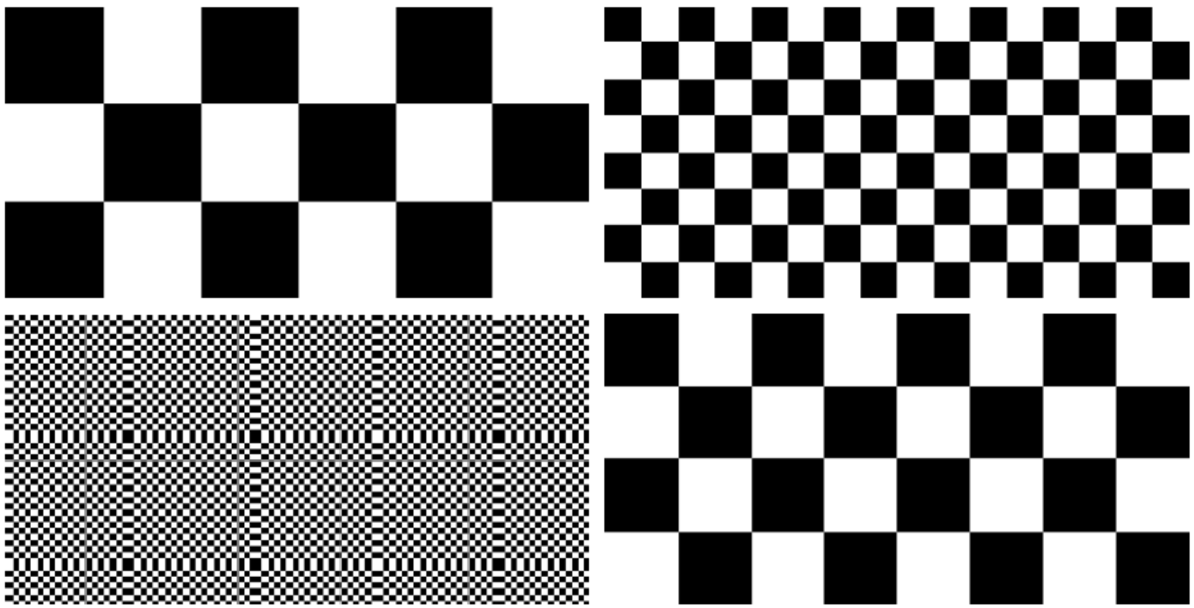

a	b
c	d

FIGURE 4.16 Aliasing in images. In (a) and (b), the lengths of the sides of the squares are 16 and 6 pixels, respectively, and aliasing is visually negligible. In (c) and (d), the sides of the squares are 0.9174 and 0.4798 pixels, respectively, and the results show significant aliasing. Note that (d) masquerades as a “normal” image.

© 1992–2008 R. C. Gonzalez & R. E. Woods

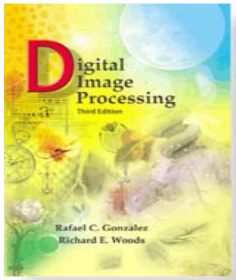

a b c

FIGURE 4.17 Illustration of aliasing on resampled images. (a) A digital image with negligible visual aliasing. (b) Result of resizing the image to 50% of its original size by pixel deletion. Aliasing is clearly visible. (c) Result of blurring the image in (a) with a 3×3 averaging filter prior to resizing. The image is slightly more blurred than (b), but aliasing is not longer objectionable. (Original image courtesy of the Signal Compression Laboratory, University of California, Santa Barbara.)

© 1992–2008 R. C. Gonzalez & R. E. Woods

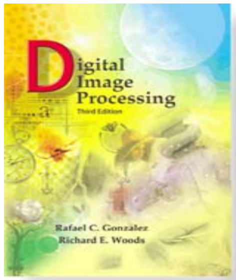

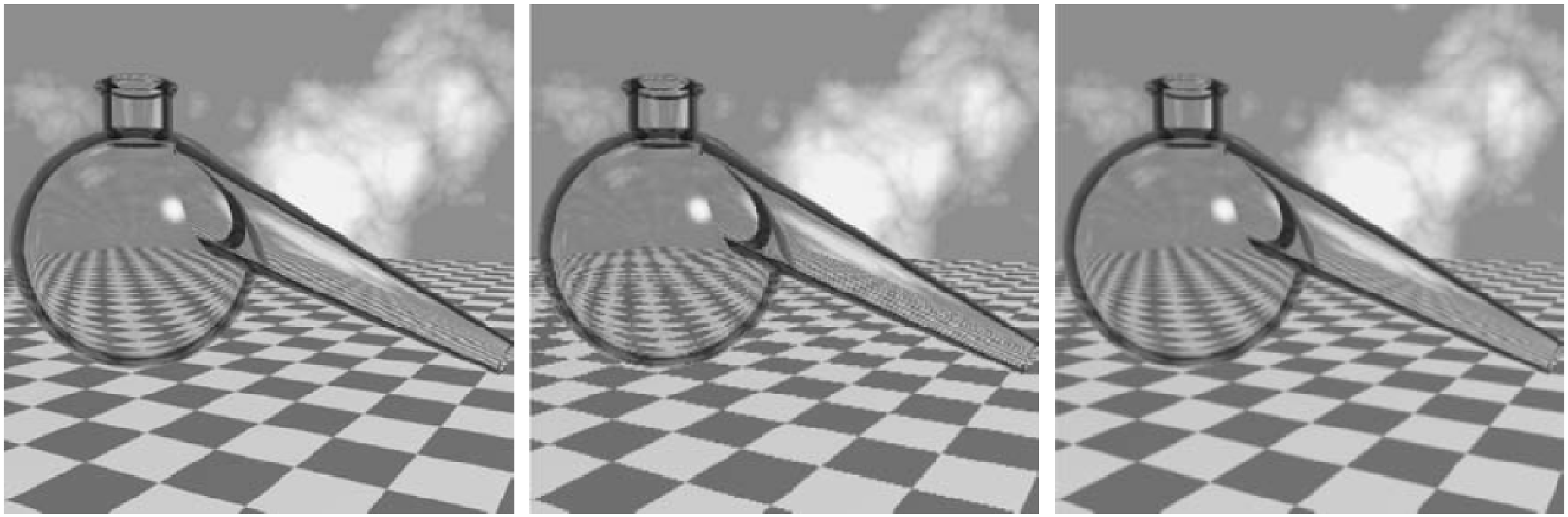

a b c

FIGURE 4.18 Illustration of jaggies. (a) A 1024 × 1024 digital image of a computer-generated scene with negligible visible aliasing. (b) Result of reducing (a) to 25% of its original size using bilinear interpolation. (c) Result of blurring the image in (a) with a 5 × 5 averaging filter prior to resizing it to 25% using bilinear interpolation. (Original image courtesy of D. P. Mitchell, Mental Landscape, LLC.)

© 1992–2008 R. C. Gonzalez & R. E. Woods

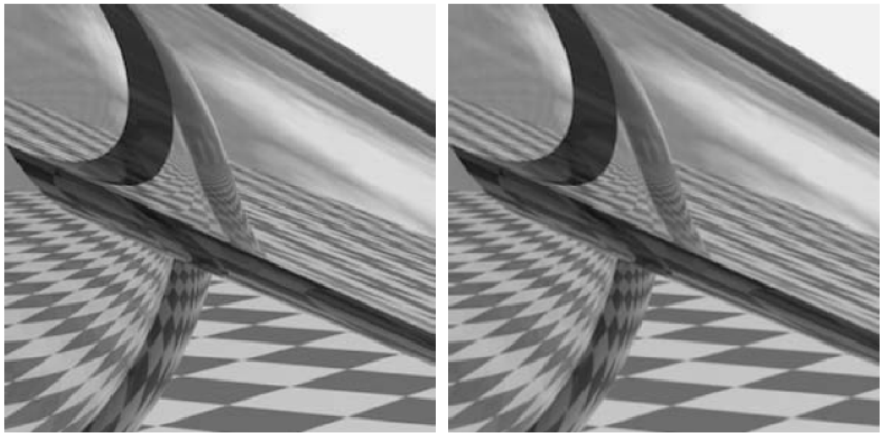

a b

FIGURE 4.19 Image zooming. (a) A 1024×1024 digital image generated by pixel replication from a 256×256 image extracted from the middle of Fig. 4.18(a). (b) Image generated using bi-linear interpolation, showing a significant reduction in jaggies.

© 1992–2008 R. C. Gonzalez & R. E. Woods

Examples of Moire effect

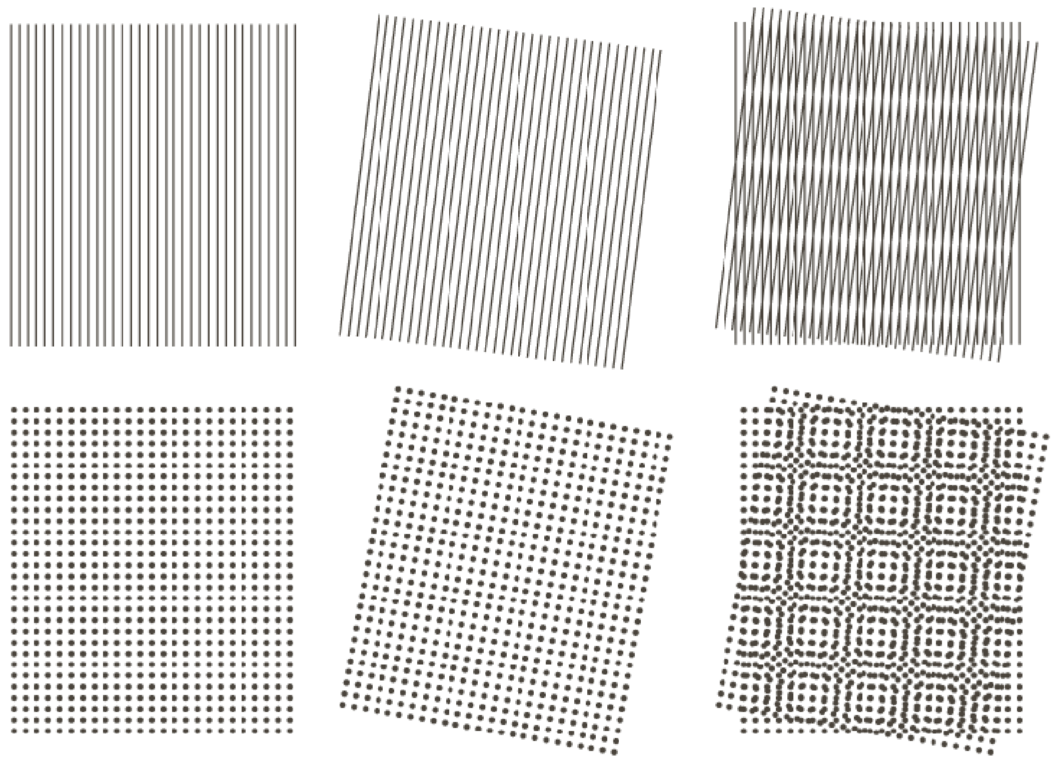

© 1992–2008 R. C. Gonzalez & R. E. Woods

Chapter 4
Filtering in the Frequency Domain

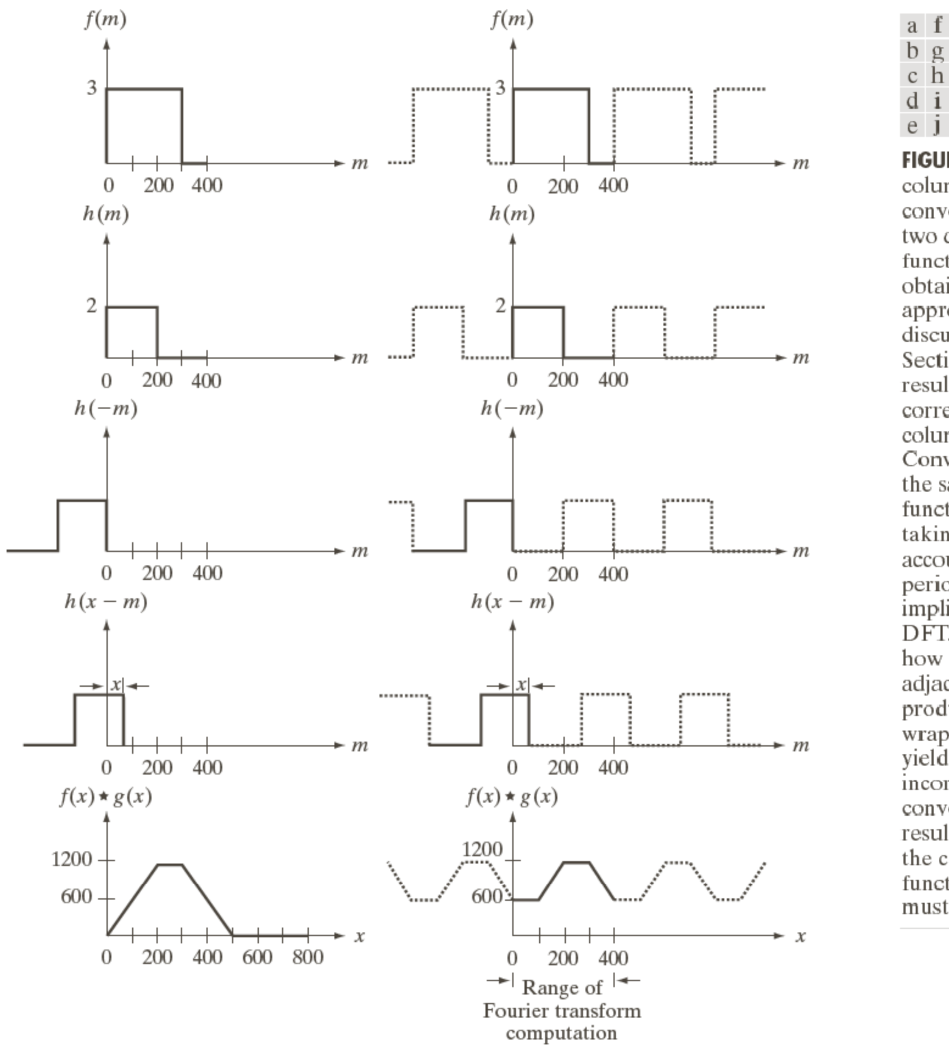

FIGURE 4.28 Left column: convolution of two discrete functions obtained using the approach discussed in Section 3.4.2. The result in (e) is correct. Right column: Convolution of the same functions, but taking into account the periodicity implied by the DFT. Note in (j) how data from adjacent periods produce wraparound error, yielding an incorrect convolution result. To obtain the correct result, function padding must be used.

© 1992–2008 R. C. Gonzalez & R. E. Woods

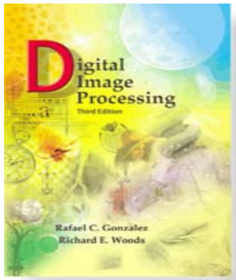

Chapter 4

Filtering in the Frequency Domain

TABLE 4.2
(Continued)

Name	Expression(s)
8) Periodicity (k_1 and k_2 are integers)	$F(u, v) = F(u + k_1M, v) = F(u, v + k_2N) = F(u + k_1M, v + k_2N)$ $f(x, y) = f(x + k_1M, y) = f(x, y + k_2N) = f(x + k_1M, y + k_2N)$
9) Convolution	$f(x, y) \bigstar h(x, y) = \sum_{m=0}^{M-1} \sum_{n=0}^{N-1} f(m, n)h(x - m, y - n)$
10) Correlation	$f(x, y) \star h(x, y) = \sum_{m=0}^{M-1} \sum_{n=0}^{N-1} f^*(m, n)h(x + m, y + n)$
11) Separability	The 2-D DFT can be computed by computing 1-D DFT transforms along the rows (columns) of the image, followed by 1-D transforms along the columns (rows) of the result. See Section 4.11.1.
12) Obtaining the inverse Fourier transform using a forward transform algorithm.	$MNf^*(x, y) = \sum_{u=0}^{M-1} \sum_{v=0}^{N-1} F^*(u, v)e^{-j2\pi(ux/M + vy/N)}$ This equation indicates that inputting $F^*(u, v)$ into an algorithm that computes the forward transform (right side of above equation) yields $MNf^*(x, y)$. Taking the complex conjugate and dividing by MN gives the desired inverse. See Section 4.11.2.

© 1992–2008 R. C. Gonzalez & R. E. Woods

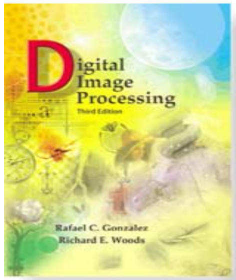

Name	DFT Pairs
1) Symmetry properties	See Table 4.1
2) Linearity	$af_1(x, y) + bf_2(x, y) \Leftrightarrow aF_1(u, v) + bF_2(u, v)$
3) Translation (general)	$f(x, y)e^{j2\pi(u_0x/M + v_0y/N)} \Leftrightarrow F(u - u_0, v - v_0)$ $f(x - x_0, y - y_0) \Leftrightarrow F(u, v)e^{-j2\pi(ux_0/M + vy_0/N)}$
4) Translation to center of the frequency rectangle, $(M/2, N/2)$	$f(x, y)(-1)^{x+y} \Leftrightarrow F(u - M/2, v - N/2)$ $f(x - M/2, y - N/2) \Leftrightarrow F(u, v)(-1)^{u+v}$
5) Rotation	$f(r, \theta + \theta_0) \Leftrightarrow F(\omega, \varphi + \theta_0)$ $x = r\cos\theta \quad y = r\sin\theta \quad u = \omega\cos\varphi \quad v = \omega\sin\varphi$
6) Convolution theorem†	$f(x, y) \star h(x, y) \Leftrightarrow F(u, v)H(u, v)$ $f(x, y)h(x, y) \Leftrightarrow F(u, v) \star H(u, v)$

(*Continued*)

TABLE 4.3
Summary of DFT pairs. The closed-form expressions in 12 and 13 are valid only for continuous variables. They can be used with discrete variables by sampling the closed-form, continuous expressions.

© 1992–2008 R. C. Gonzalez & R. E. Woods

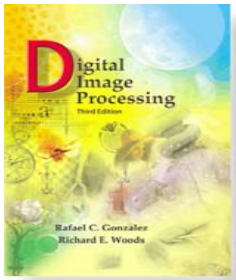

TABLE 4.3 (*Continued*)

Name	DFT Pairs
7) Correlation theorem†	$f(x,y) \star h(x,y) \Leftrightarrow F^*(u,v)\,H(u,v)$ $f^*(x,y)h(x,y) \Leftrightarrow F(u,v) \star H(u,v)$
8) Discrete unit impulse	$\delta(x,y) \Leftrightarrow 1$
9) Rectangle	$\text{rect}[a,b] \Leftrightarrow ab\dfrac{\sin(\pi ua)}{(\pi ua)}\dfrac{\sin(\pi vb)}{(\pi vb)}e^{-j\pi(ua+vb)}$
10) Sine	$\sin(2\pi u_0 x + 2\pi v_0 y) \Leftrightarrow$ $j\frac{1}{2}\left[\delta(u+Mu_0, v+Nv_0) - \delta(u-Mu_0, v-Nv_0)\right]$
11) Cosine	$\cos(2\pi u_0 x + 2\pi v_0 y) \Leftrightarrow$ $\frac{1}{2}\left[\delta(u+Mu_0, v+Nv_0) + \delta(u-Mu_0, v-Nv_0)\right]$

The following Fourier transform pairs are derivable only for continuous variables, denoted as before by t and z for spatial variables and by μ and ν for frequency variables. These results can be used for DFT work by sampling the continuous forms.

12) *Differentiation* (The expressions on the right assume that $f(\pm\infty, \pm\infty) = 0$.)	$\left(\dfrac{\partial}{\partial t}\right)^m\left(\dfrac{\partial}{\partial z}\right)^n f(t,z) \Leftrightarrow (j2\pi\mu)^m(j2\pi\nu)^n F(\mu,\nu)$ $\dfrac{\partial^m f(t,z)}{\partial t^m} \Leftrightarrow (j2\pi\mu)^m F(\mu,\nu);\ \dfrac{\partial^n f(t,z)}{\partial z^n} \Leftrightarrow (j2\pi\nu)^n F(\mu,\nu)$
13) *Gaussian*	$A2\pi\sigma^2 e^{-2\pi^2\sigma^2(t^2+z^2)} \Leftrightarrow Ae^{-(\mu^2+\nu^2)/2\sigma^2}$ (A is a constant)

†Assumes that the functions have been extended by zero padding. Convolution and correlation are associative, commutative, and distributive.

© 1992–2008 R. C. Gonzalez & R. E. Woods

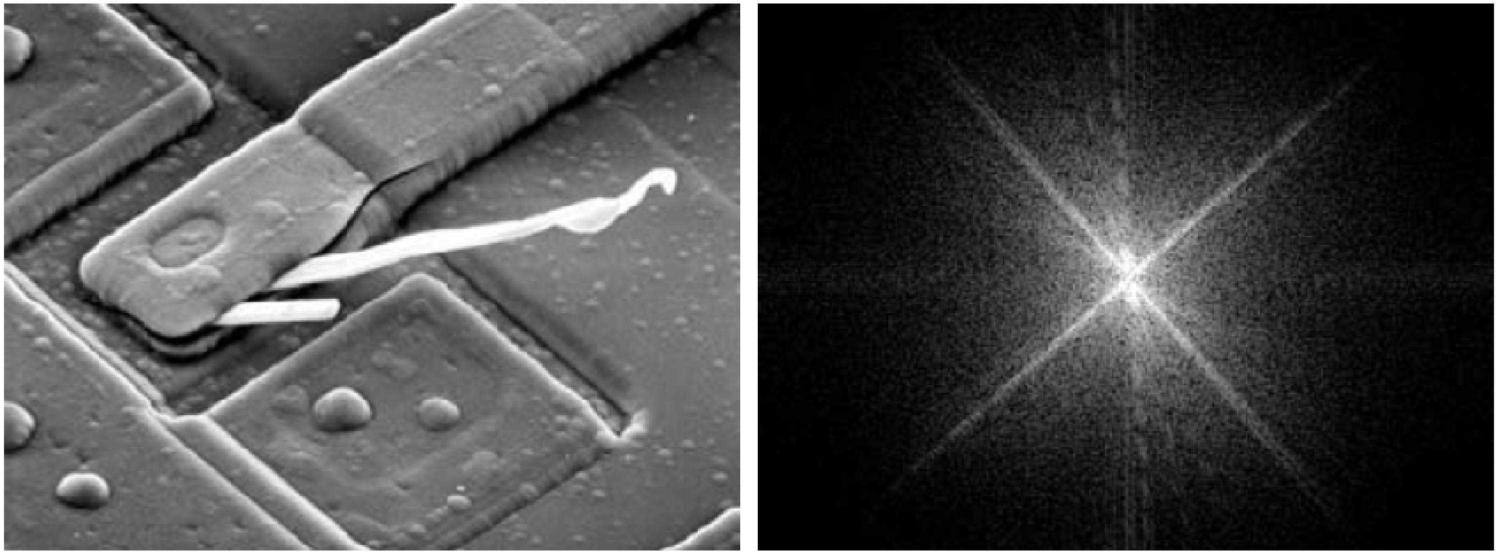

a b

FIGURE 4.29 (a) SEM image of a damaged integrated circuit. (b) Fourier spectrum of (a). (Original image courtesy of Dr. J. M. Hudak, Brockhouse Institute for Materials Research, McMaster University, Hamilton, Ontario, Canada.)

© 1992–2008 R. C. Gonzalez & R. E. Woods

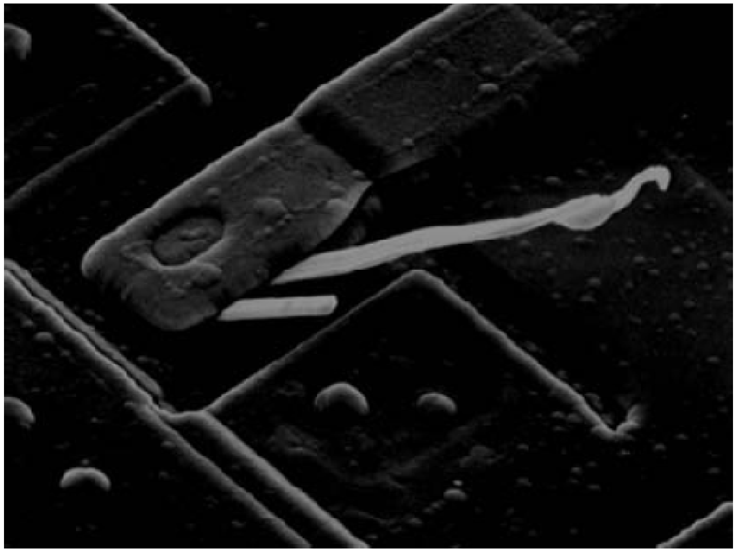

FIGURE 4.30 Result of filtering the image in Fig. 4.29(a) by setting to 0 the term $F(M/2, N/2)$ in the Fourier transform.

© 1992–2008 R. C. Gonzalez & R. E. Woods

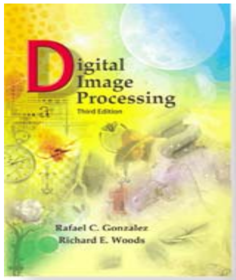

Chapter 4
Filtering in the Frequency Domain

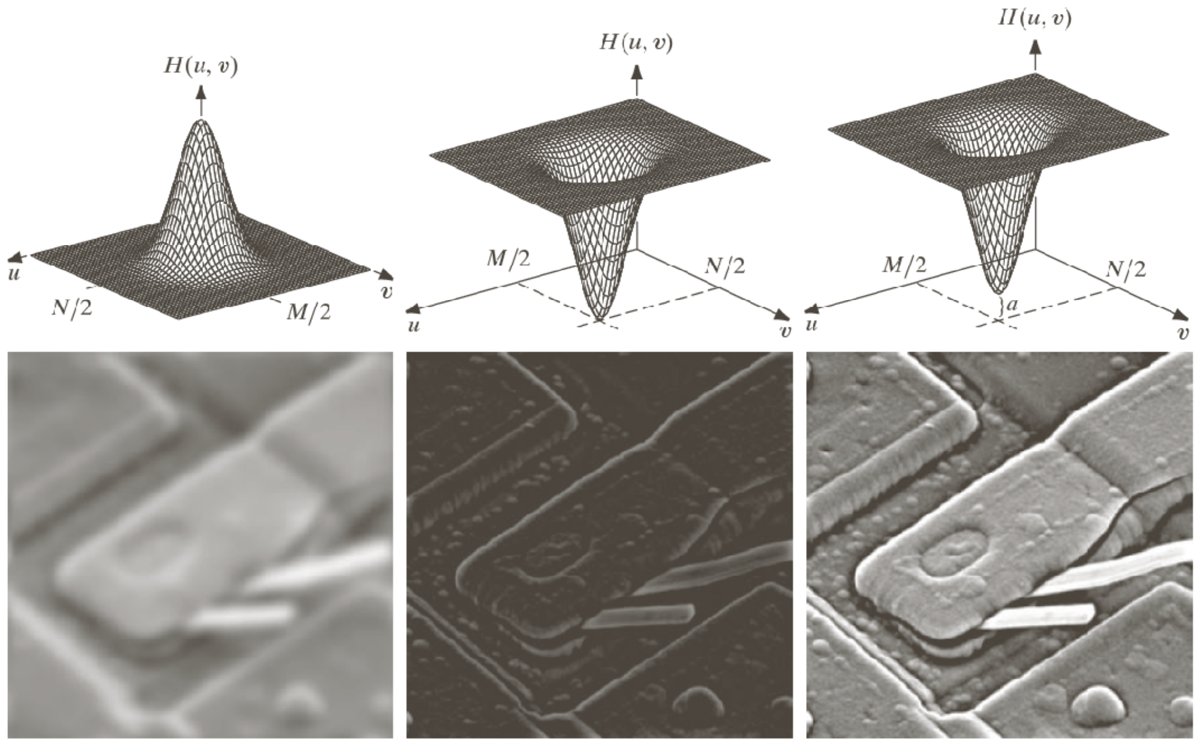

a b c
d e f

FIGURE 4.31 Top row: frequency domain filters. Bottom row: corresponding filtered images obtained using Eq. (4.7-1). We used $a = 0.85$ in (c) to obtain (f) (the height of the filter itself is 1). Compare (f) with Fig. 4.29(a).

© 1992–2008 R. C. Gonzalez & R. E. Woods

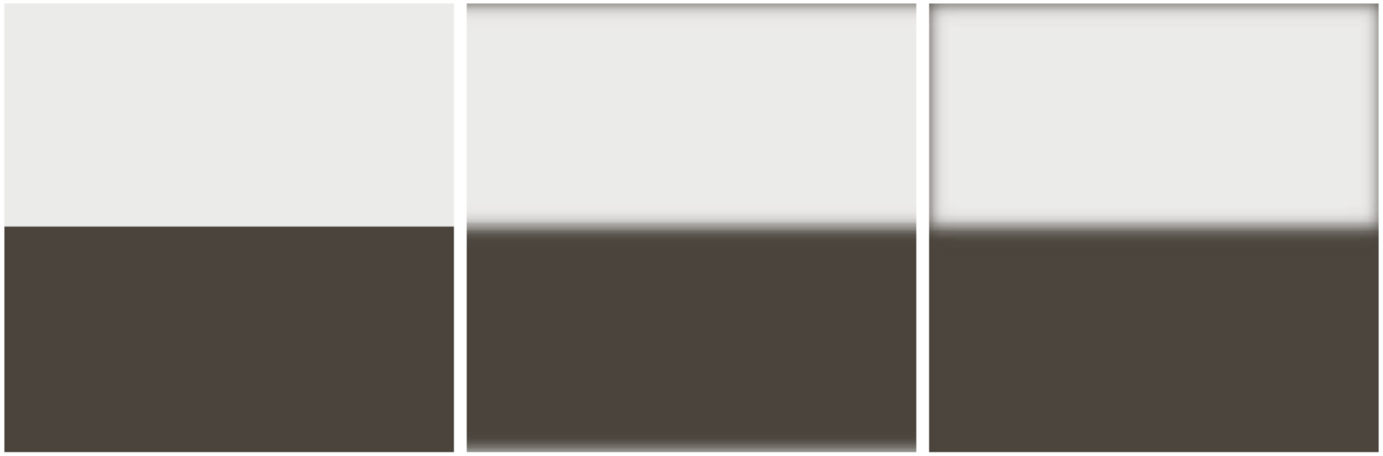

a b c

FIGURE 4.32 (a) A simple image. (b) Result of blurring with a Gaussian lowpass filter without padding. (c) Result of lowpass filtering with padding. Compare the light area of the vertical edges in (b) and (c).

© 1992–2008 R. C. Gonzalez & R. E. Woods

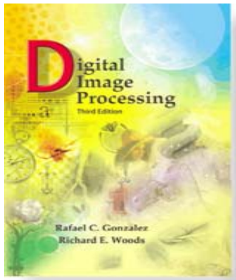

Chapter 4
Filtering in the Frequency Domain

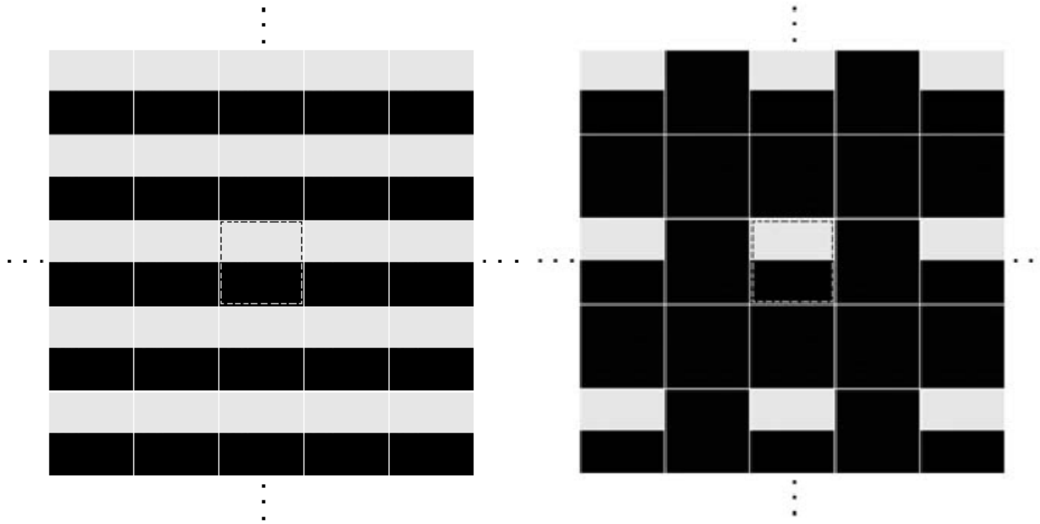

a b

FIGURE 4.33 2-D image periodicity inherent in using the DFT. (a) Periodicity without image padding. (b) Periodicity after padding with 0s (black). The dashed areas in the center correspond to the image in Fig. 4.32(a). (The thin white lines in both images are superimposed for clarity; they are not part of the data.)

© 1992–2008 R. C. Gonzalez & R. E. Woods

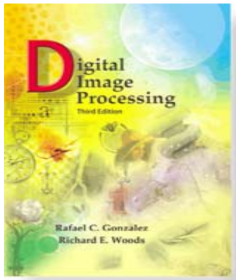

Chapter 4
Filtering in the Frequency Domain

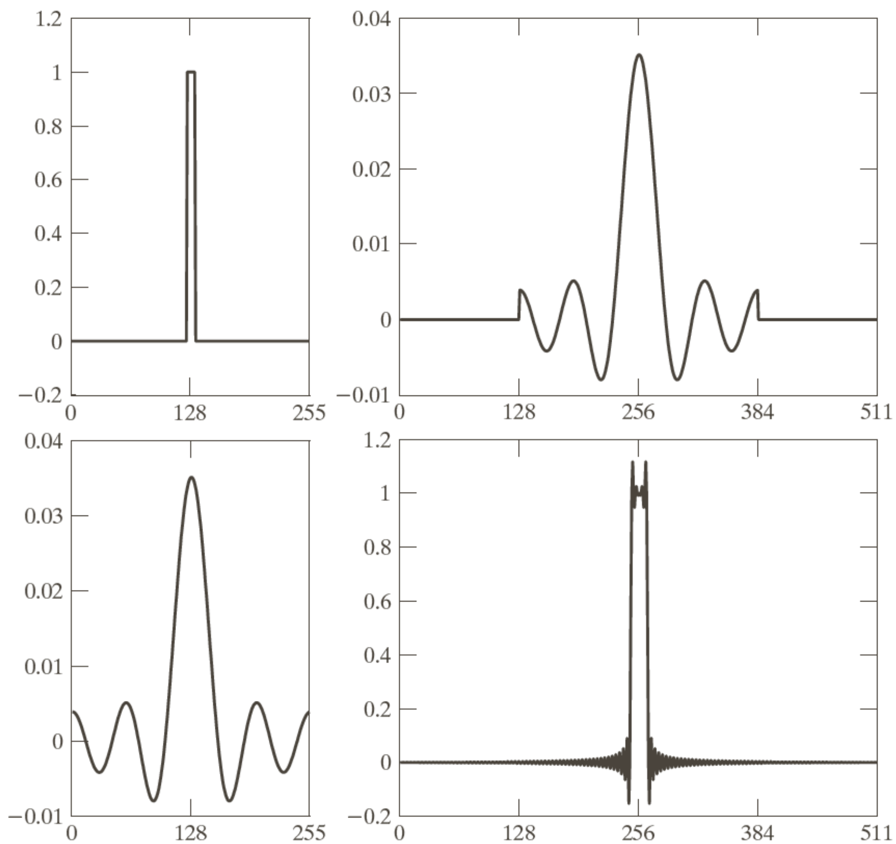

a c
b d

FIGURE 4.34 (a) Original filter specified in the (centered) frequency domain. (b) Spatial representation obtained by computing the IDFT of (a). (c) Result of padding (b) to twice its length (note the discontinuities). (d) Corresponding filter in the frequency domain obtained by computing the DFT of (c). Note the ringing caused by the discontinuities in (c). (The curves appear continuous because the points were joined to simplify visual analysis.)

© 1992–2008 R. C. Gonzalez & R. E. Woods

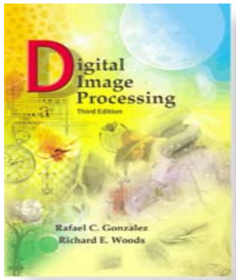

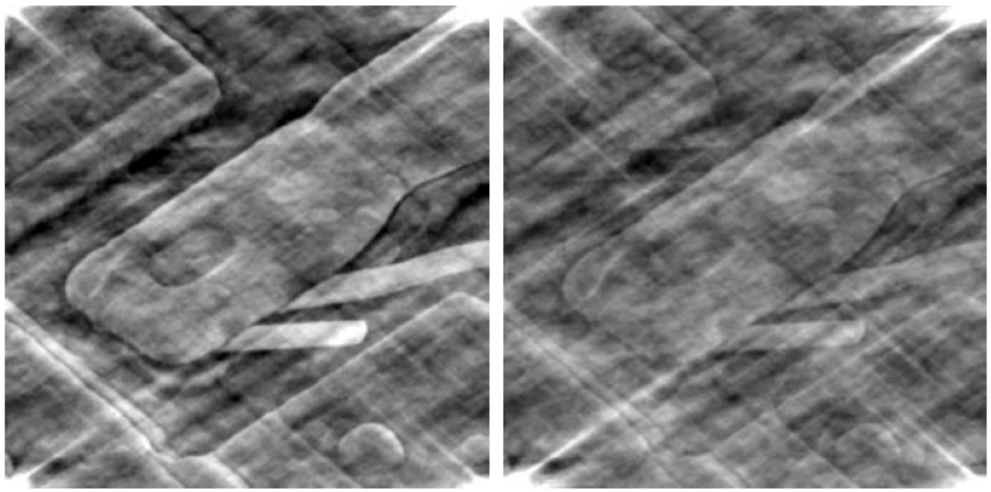

a b

FIGURE 4.35 (a) Image resulting from multiplying by 0.5 the phase angle in Eq. (4.6-15) and then computing the IDFT. (b) The result of multiplying the phase by 0.25. The spectrum was not changed in either of the two cases.

© 1992–2008 R. C. Gonzalez & R. E. Woods

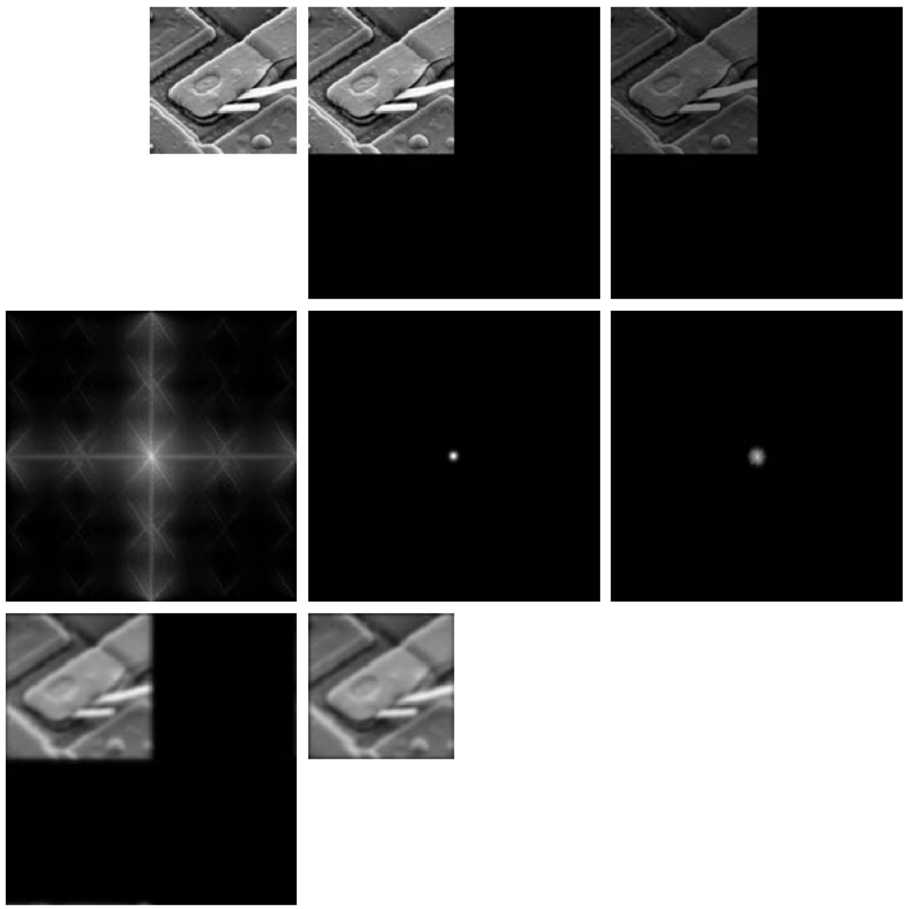

a b c
d e f
g h

FIGURE 4.36 (a) An $M \times N$ image, f. (b) Padded image, f_p of size $P \times Q$. (c) Result of multiplying f_p by $(-1)^{x+y}$. (d) Spectrum of F_p. (e) Centered Gaussian lowpass filter, H, of size $P \times Q$. (f) Spectrum of the product HF_p. (g) g_p, the product of $(-1)^{x+y}$ and the real part of the IDFT of HF_p. (h) Final result, g, obtained by cropping the first M rows and N columns of g_p.

© 1992–2008 R. C. Gonzalez & R. E. Woods

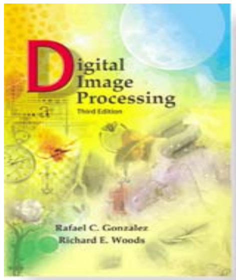

Chapter 4
Filtering in the Frequency Domain

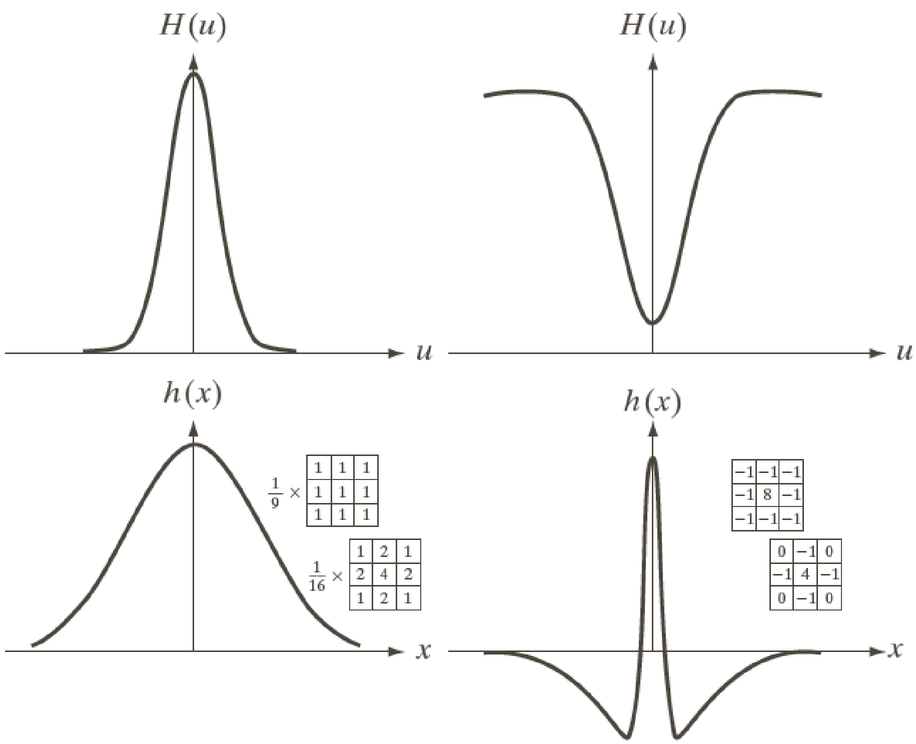

a c
b d

FIGURE 4.37 (a) A 1-D Gaussian lowpass filter in the frequency domain. (b) Spatial lowpass filter corresponding to (a). (c) Gaussian highpass filter in the frequency domain. (d) Spatial highpass filter corresponding to (c). The small 2-D masks shown are spatial filters we used in Chapter 3.

© 1992–2008 R. C. Gonzalez & R. E. Woods

Chapter 4
Filtering in the Frequency Domain

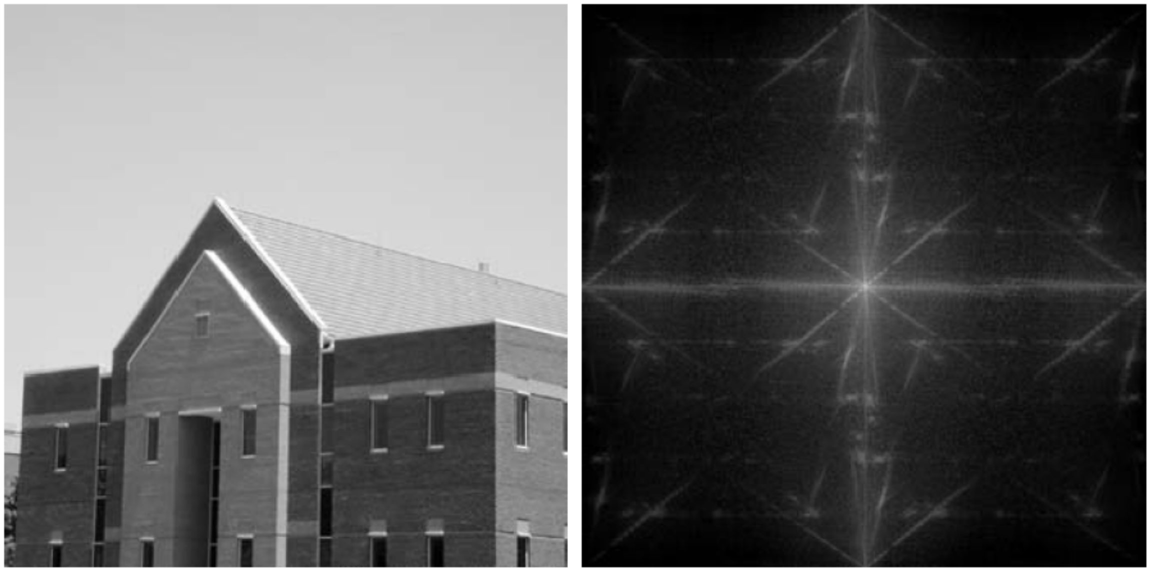

a b

FIGURE 4.38
(a) Image of a building, and (b) its spectrum.

© 1992–2008 R. C. Gonzalez & R. E. Woods

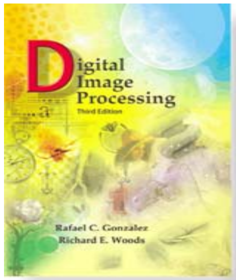

Chapter 4
Filtering in the Frequency Domain

−1	0	1
−2	0	2
−1	0	1

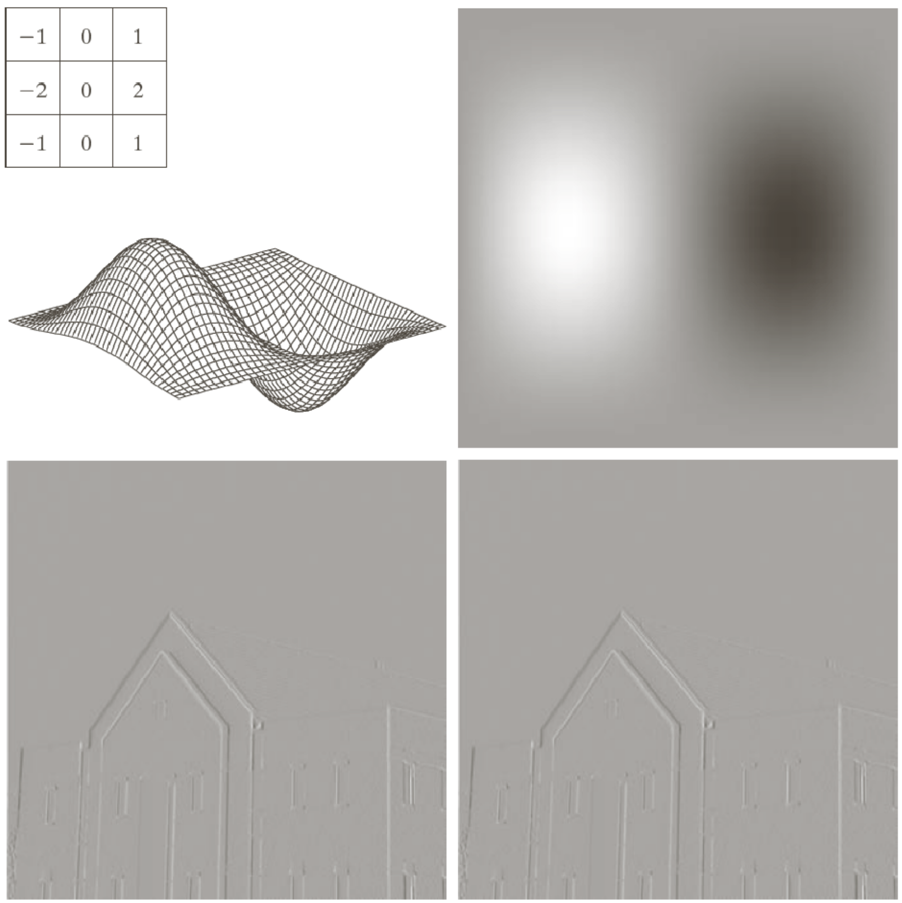

a b
c d

FIGURE 4.39 (a) A spatial mask and perspective plot of its corresponding frequency domain filter. (b) Filter shown as an image. (c) Result of filtering Fig. 4.38(a) in the frequency domain with the filter in (b). (d) Result of filtering the same image with the spatial filter in (a). The results are identical.

© 1992–2008 R. C. Gonzalez & R. E. Woods

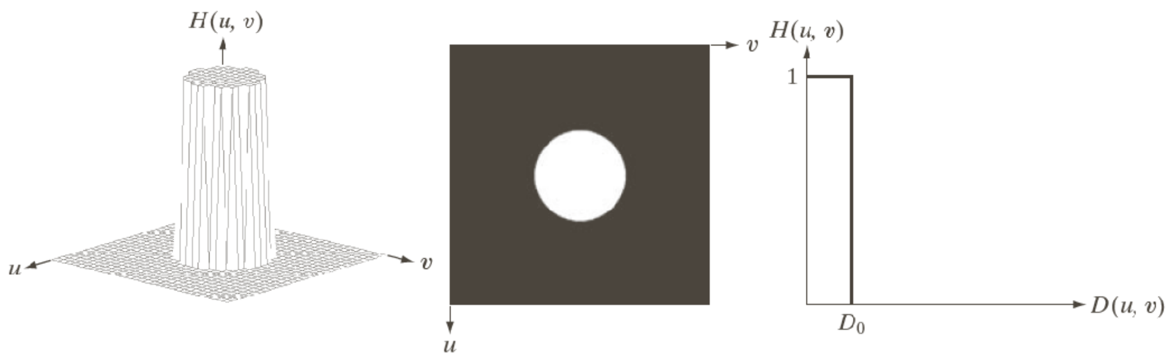

FIGURE 4.40 (a) Perspective plot of an ideal lowpass-filter transfer function. (b) Filter displayed as an image. (c) Filter radial cross section.

© 1992–2008 R. C. Gonzalez & R. E. Woods

Chapter 4

Filtering in the Frequency Domain

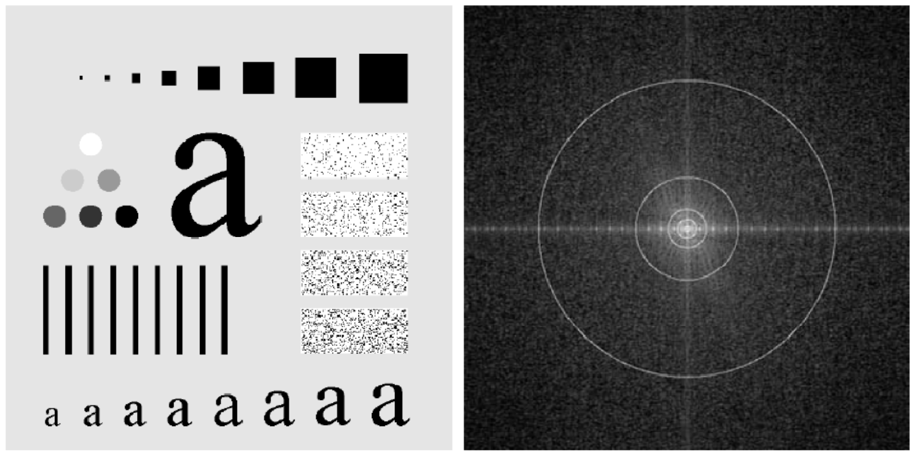

a b

FIGURE 4.41 (a) Test pattern of size 688 × 688 pixels, and (b) its Fourier spectrum. The spectrum is double the image size due to padding but is shown in half size so that it fits in the page. The superimposed circles have radii equal to 10, 30, 60, 160, and 460 with respect to the full-size spectrum image. These radii enclose 87.0, 93.1, 95.7, 97.8, and 99.2% of the padded image power, respectively.

© 1992–2008 R. C. Gonzalez & R. E. Woods

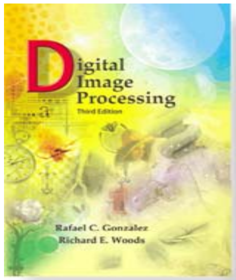

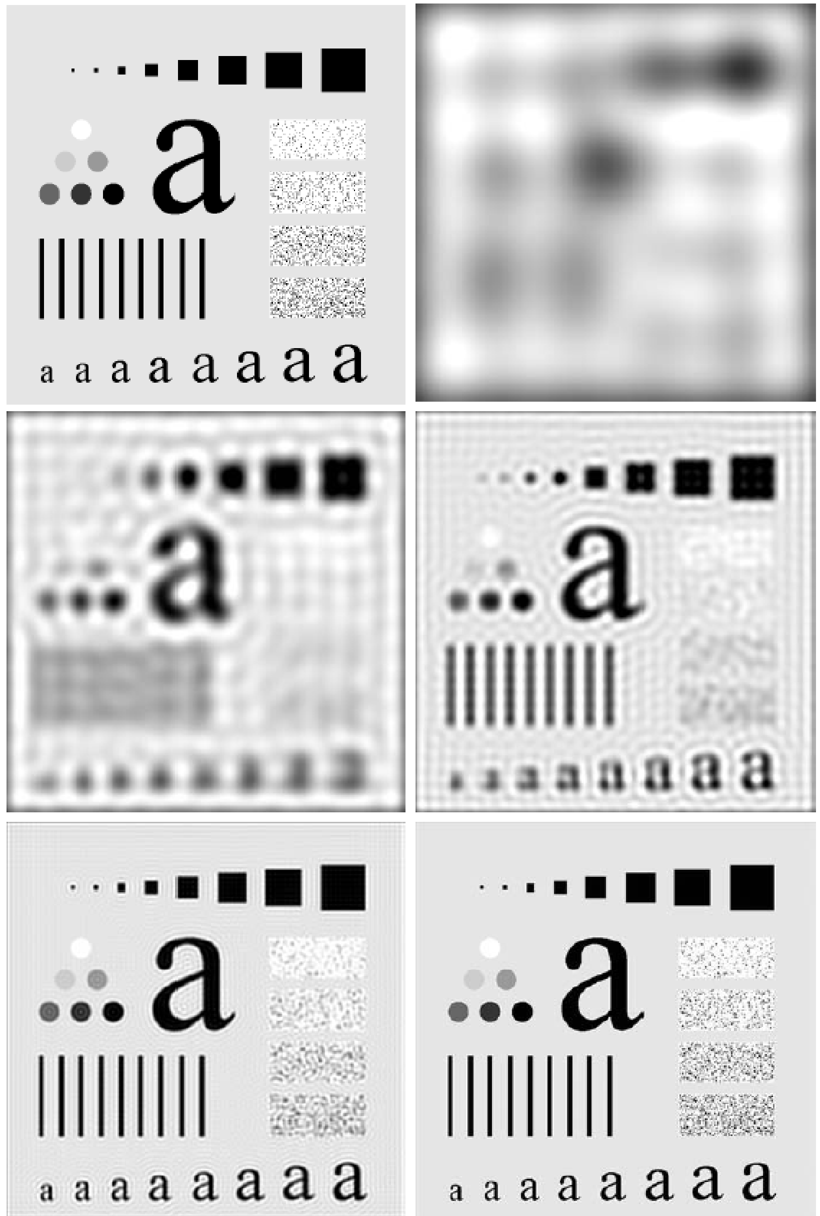

a b
c d
e f

FIGURE 4.42 (a) Original image. (b)–(f) Results of filtering using ILPFs with cutoff frequencies set at radii values 10, 30, 60, 160, and 460, as shown in Fig. 4.41(b). The power removed by these filters was 13, 6.9, 4.3, 2.2, and 0.8% of the total, respectively.

© 1992–2008 R. C. Gonzalez & R. E. Woods

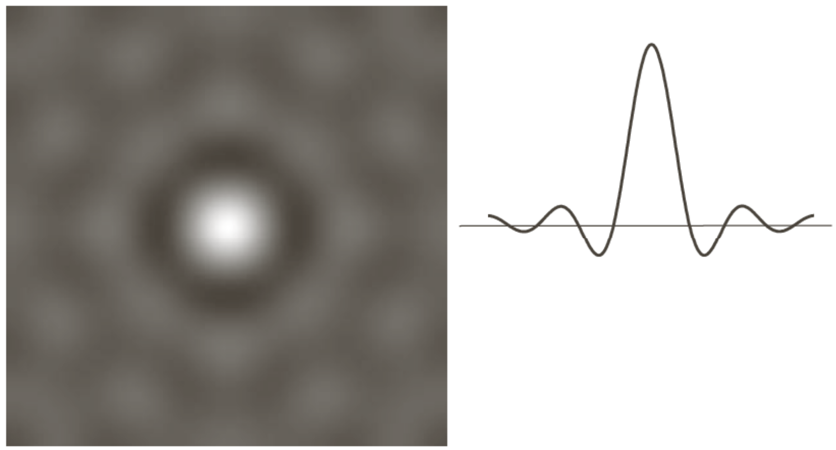

a b

FIGURE 4.43 (a) Representation in the spatial domain of an ILPF of radius 5 and size 1000×1000. (b) Intensity profile of a horizontal line passing through the center of the image.

© 1992–2008 R. C. Gonzalez & R. E. Woods

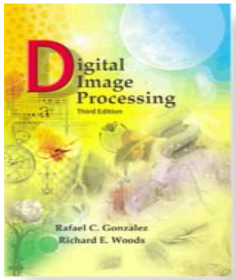

Chapter 4
Filtering in the Frequency Domain

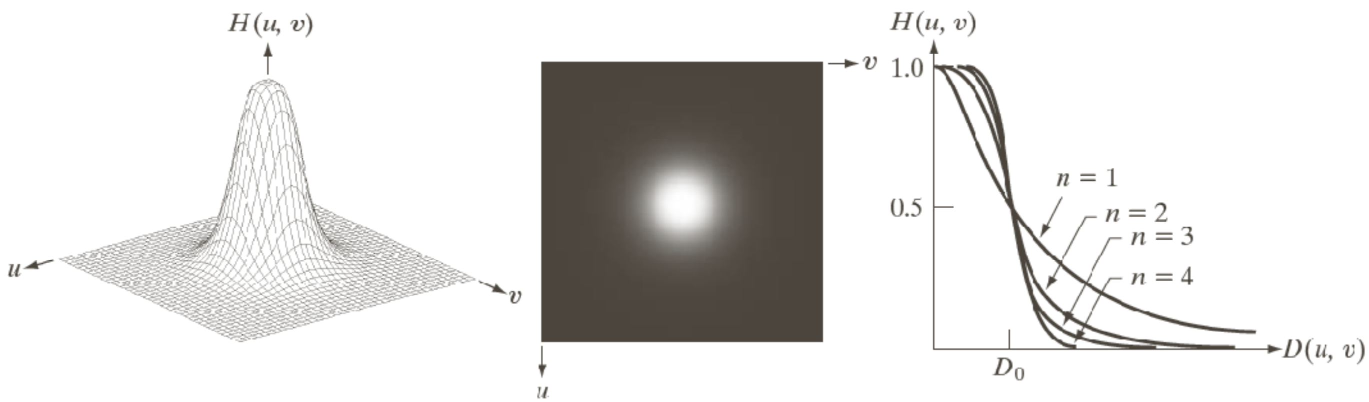

a b c

FIGURE 4.44 (a) Perspective plot of a Butterworth lowpass-filter transfer function. (b) Filter displayed as an image. (c) Filter radial cross sections of orders 1 through 4.

© 1992–2008 R. C. Gonzalez & R. E. Woods

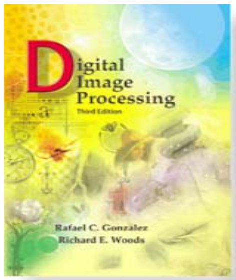

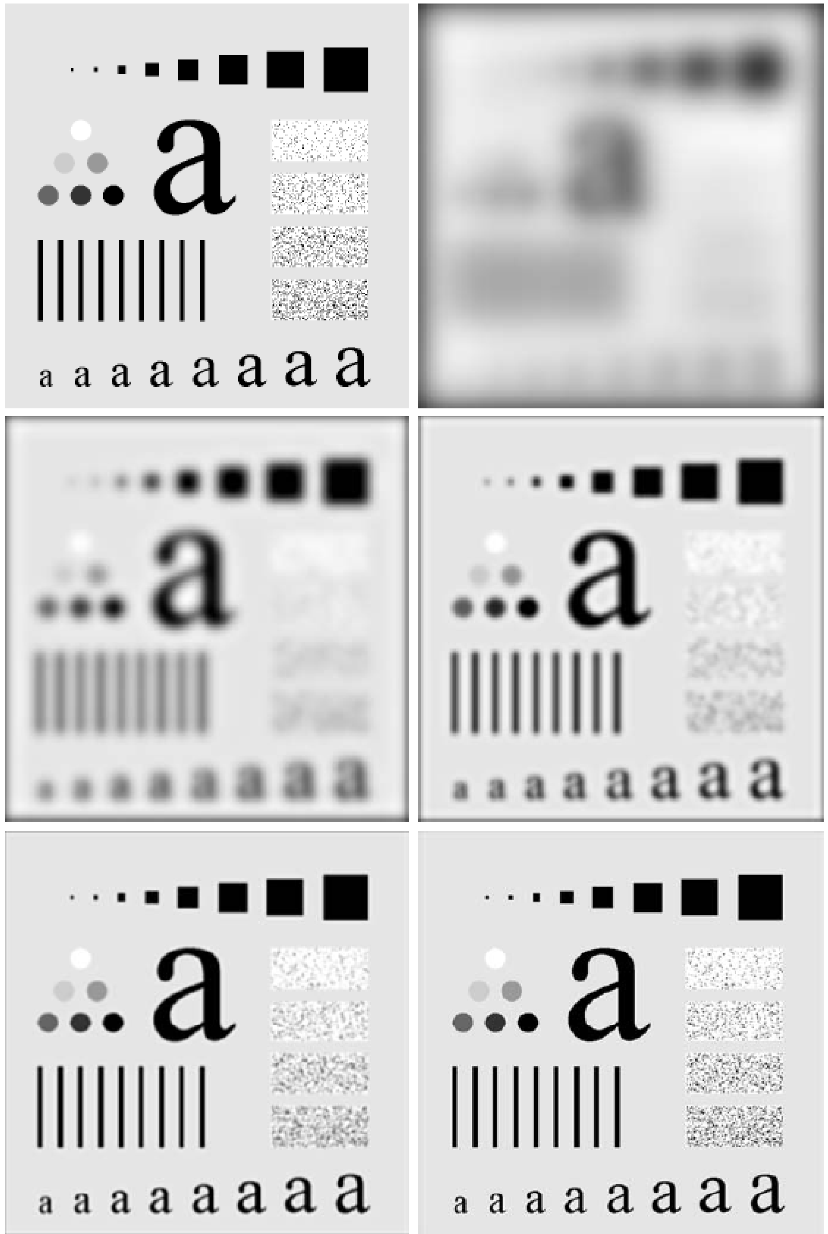

a b
c d
e f

FIGURE 4.45 (a) Original image. (b)–(f) Results of filtering using BLPFs of order 2, with cutoff frequencies at the radii shown in Fig. 4.41. Compare with Fig. 4.42.

© 1992–2008 R. C. Gonzalez & R. E. Woods

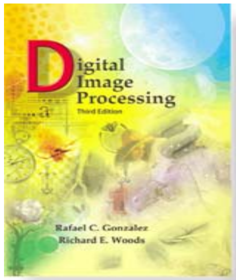

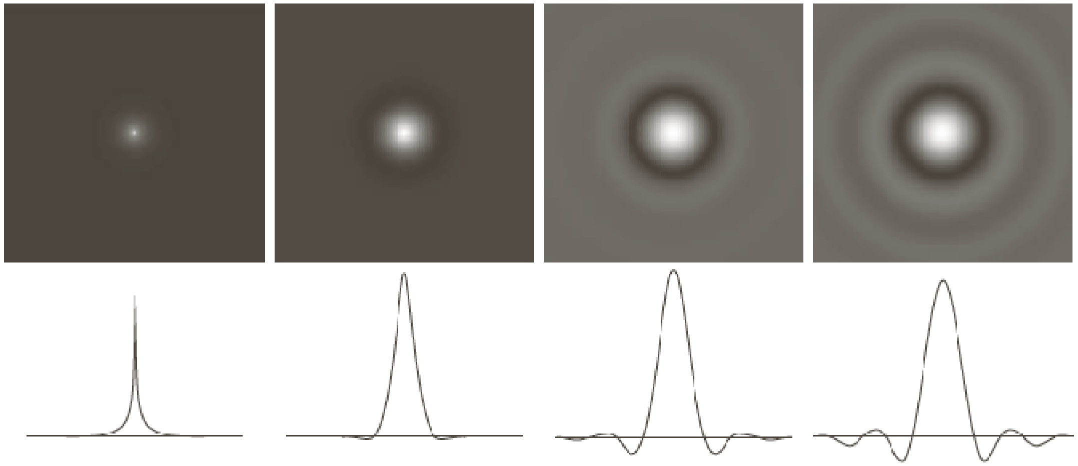

a b c d

FIGURE 4.46 (a) (d) Spatial representation of BLPFs of order 1, 2, 5, and 20, and corresponding intensity profiles through the center of the filters (the size in all cases is 1000×1000 and the cutoff frequency is 5). Observe how ringing increases as a function of filter order.

© 1992–2008 R. C. Gonzalez & R. E. Woods

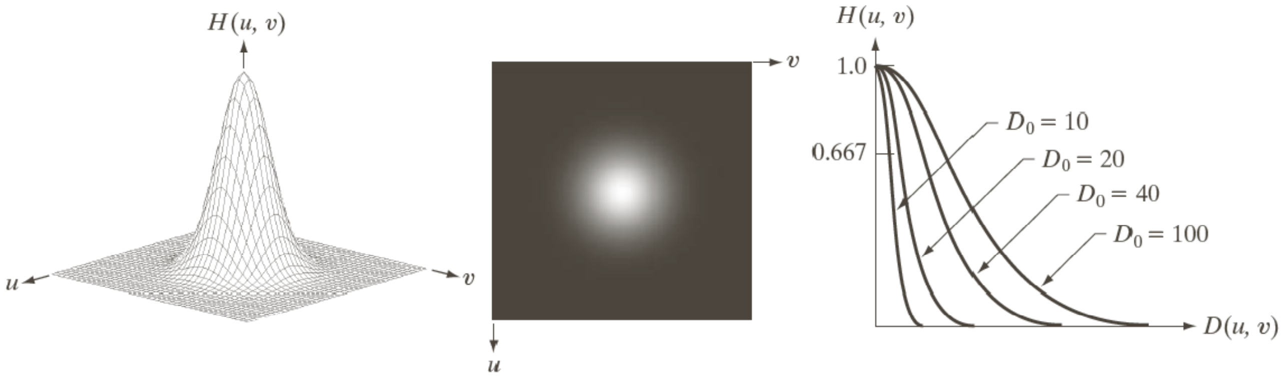

FIGURE 4.47 (a) Perspective plot of a GLPF transfer function. (b) Filter displayed as an image. (c) Filter radial cross sections for various values of D_0.

© 1992–2008 R. C. Gonzalez & R. E. Woods

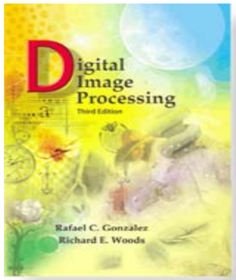

TABLE 4.4
Lowpass filters. D_0 is the cutoff frequency and n is the order of the Butterworth filter.

Ideal	Butterworth	Gaussian
$H(u,v) = \begin{cases} 1 & \text{if } D(u,v) \leq D_0 \\ 0 & \text{if } D(u,v) > D_0 \end{cases}$	$H(u,v) = \dfrac{1}{1 + [D(u,v)/D_0]^{2n}}$	$H(u,v) = e^{-D^2(u,v)/2D_0^2}$

© 1992–2008 R. C. Gonzalez & R. E. Woods

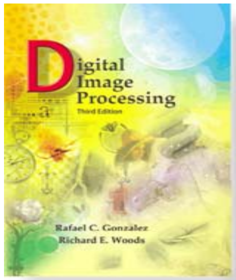

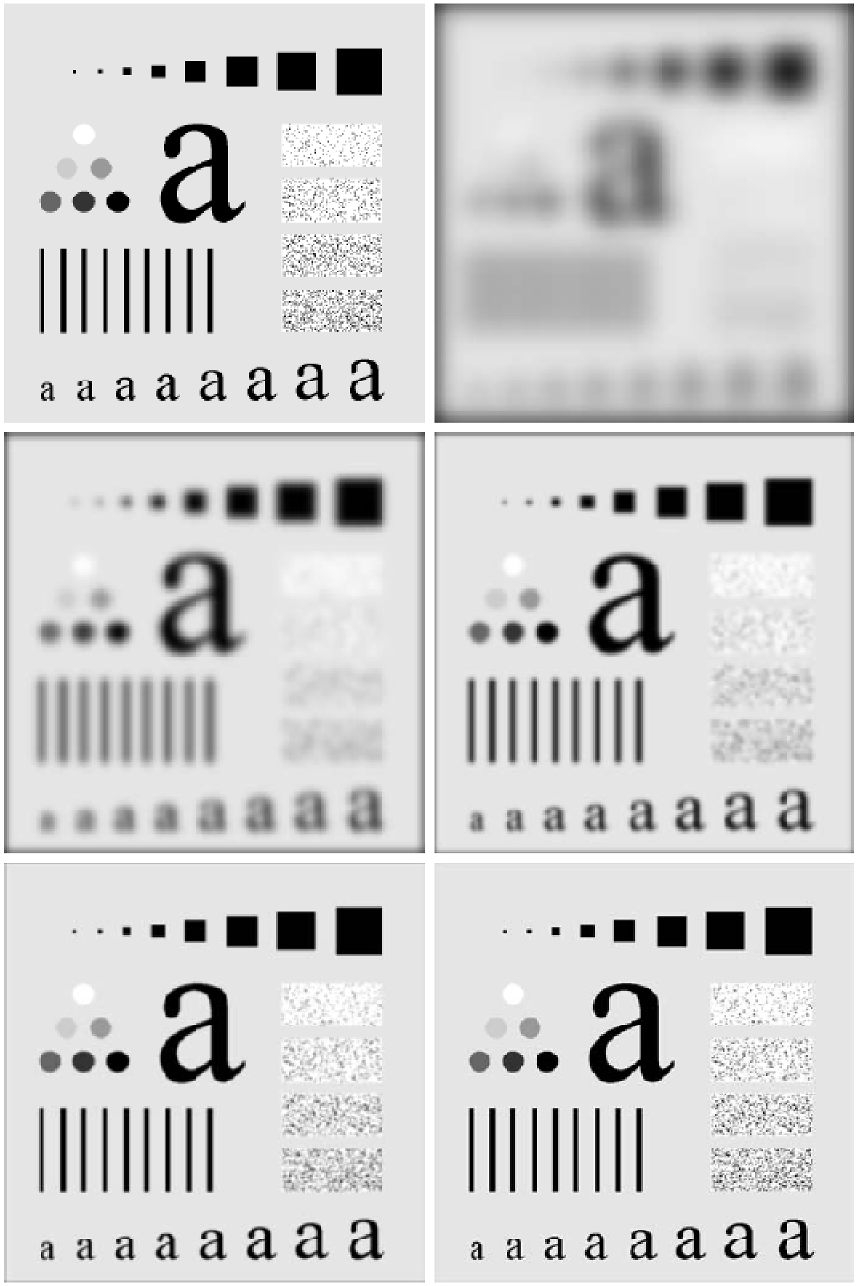

a b
c d
e f

FIGURE 4.48 (a) Original image. (b)–(f) Results of filtering using GLPFs with cutoff frequencies at the radii shown in Fig. 4.41. Compare with Figs. 4.42 and 4.45.

© 1992–2008 R. C. Gonzalez & R. E. W

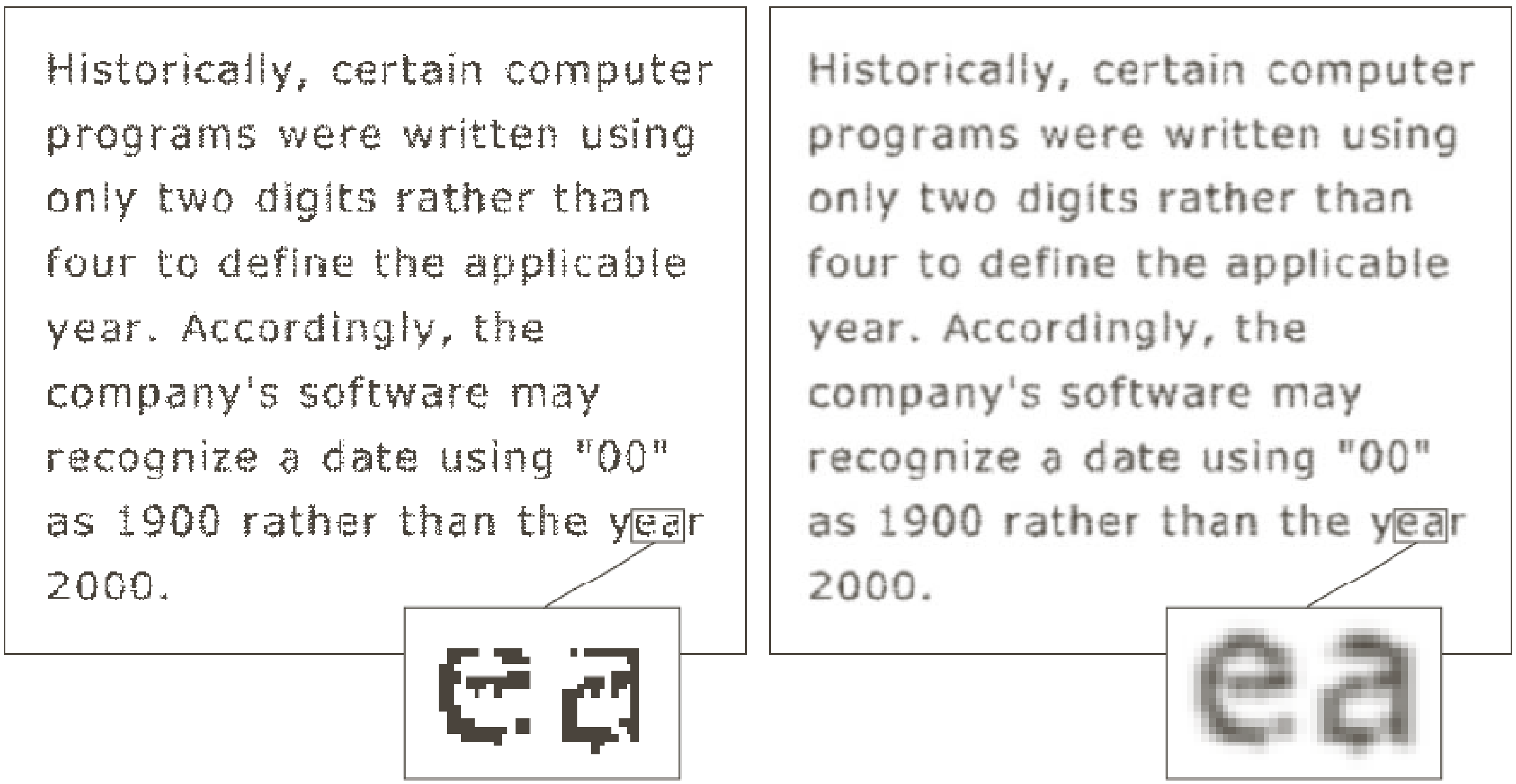

Historically, certain computer programs were written using only two digits rather than four to define the applicable year. Accordingly, the company's software may recognize a date using "00" as 1900 rather than the year 2000.

Historically, certain computer programs were written using only two digits rather than four to define the applicable year. Accordingly, the company's software may recognize a date using "00" as 1900 rather than the year 2000.

© 1992–2008 R. C. Gonzalez & R. E. Woods

a b c

FIGURE 4.50 (a) Original image (784 × 732 pixels). (b) Result of filtering using a GLPF with $D_0 = 100$. (c) Result of filtering using a GLPF with $D_0 = 80$. Note the reduction in fine skin lines in the magnified sections in (b) and (c).

© 1992–2008 R. C. Gonzalez & R. E. Woods

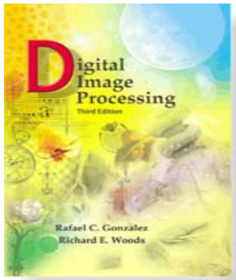

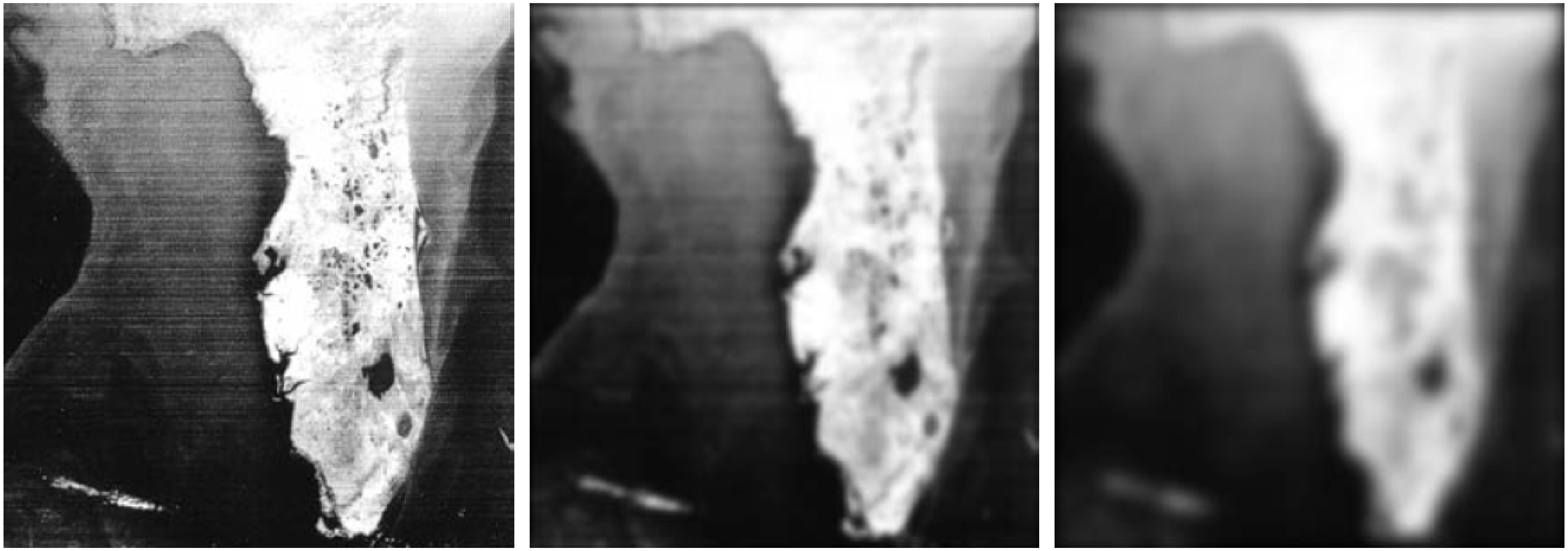

a b c

FIGURE 4.51 (a) Image showing prominent horizontal scan lines. (b) Result of filtering using a GLPF with $D_0 = 50$. (c) Result of using a GLPF with $D_0 = 20$. (Original image courtesy of NOAA.)

© 1992–2008 R. C. Gonzalez & R. E. Woods

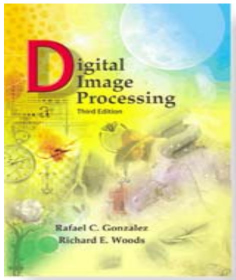

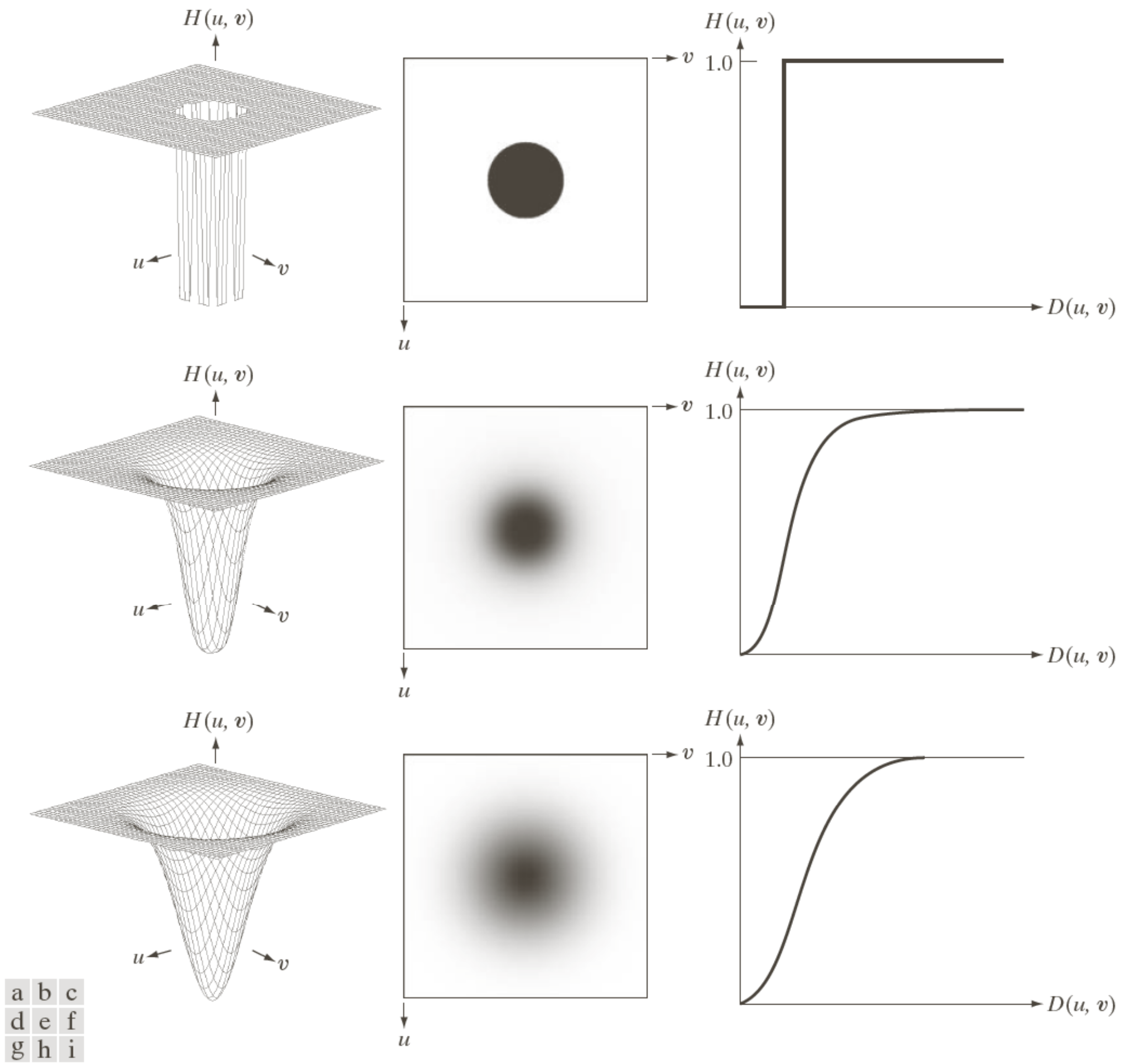

FIGURE 4.52 Top row: Perspective plot, image representation, and cross section of a typical ideal highpass filter. Middle and bottom rows: The same sequence for typical Butterworth and Gaussian highpass filters.

© 1992–2008 R. C. Gonzalez & R. E. Woods

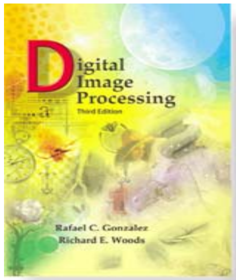

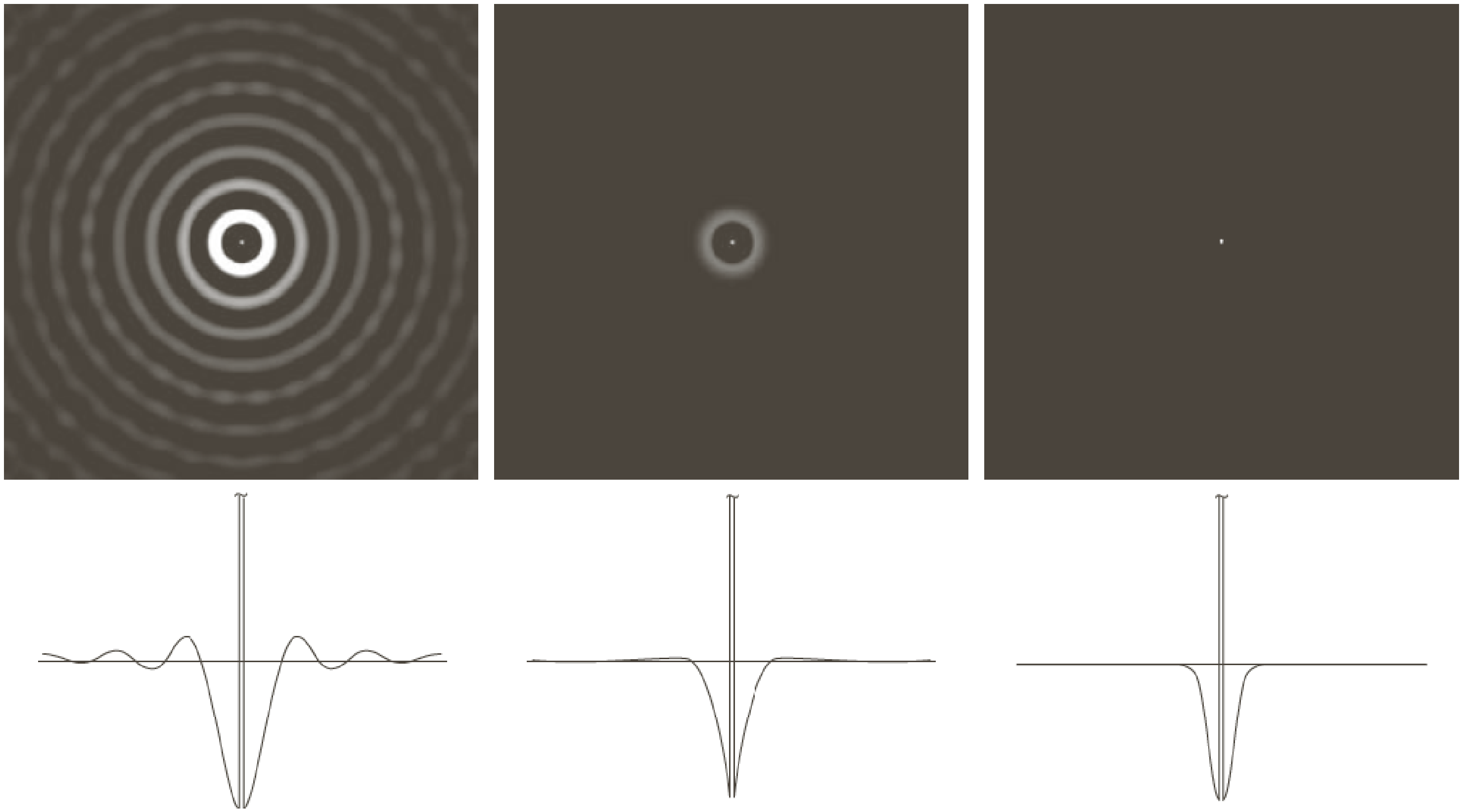

a b c

FIGURE 4.53 Spatial representation of typical (a) ideal, (b) Butterworth, and (c) Gaussian frequency domain highpass filters, and corresponding intensity profiles through their centers.

© 1992–2008 R. C. Gonzalez & R. E. Woods

a b c

FIGURE 4.54 Results of highpass filtering the image in Fig. 4.41(a) using an IHPF with $D_0 = 30$, 60, and 160.

© 1992–2008 R. C. Gonzalez & R. E. Woods

a b c

FIGURE 4.55 Results of highpass filtering the image in Fig. 4.41(a) using a BHPF of order 2 with $D_0 = 30$, 60, and 160, corresponding to the circles in Fig. 4.41(b). These results are much smoother than those obtained with an IHPF.

© 1992–2008 R. C. Gonzalez & R. E. Woods

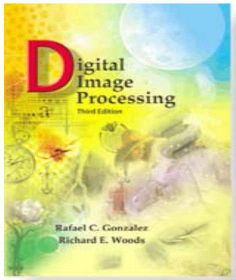

a b c

FIGURE 4.56 Results of highpass filtering the image in Fig. 4.41(a) using a GHPF with $D_0 = 30, 60$, and 160, corresponding to the circles in Fig. 4.41(b). Compare with Figs. 4.54 and 4.55.

© 1992–2008 R. C. Gonzalez & R. E. Woods

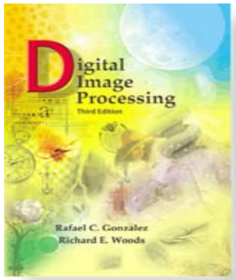

TABLE 4.5
Highpass filters. D_0 is the cutoff frequency and n is the order of the Butterworth filter.

Ideal	Butterworth	Gaussian
$H(u,v) = \begin{cases} 1 & \text{if } D(u,v) \leq D_0 \\ 0 & \text{if } D(u,v) > D_0 \end{cases}$	$H(u,v) = \dfrac{1}{1 + [D_0/D(u,v)]^{2n}}$	$H(u,v) = 1 - e^{-D^2(u,v)/2D_0^2}$

© 1992–2008 R. C. Gonzalez & R. E. Woods

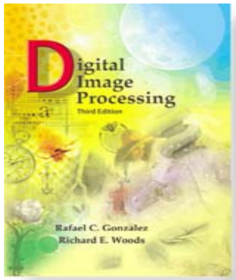

a b c

FIGURE 4.57 (a) Thumb print. (b) Result of highpass filtering (a). (c) Result of thresholding (b). (Original image courtesy of the U.S. National Institute of Standards and Technology.)

© 1992–2008 R. C. Gonzalez & R. E. Woods

a b

FIGURE 4.58 (a) Original, blurry image. (b) Image enhanced using the Laplacian in the frequency domain. Compare with Fig. 3.38(e).

© 1992–2008 R. C. Gonzalez & R. E. Woods

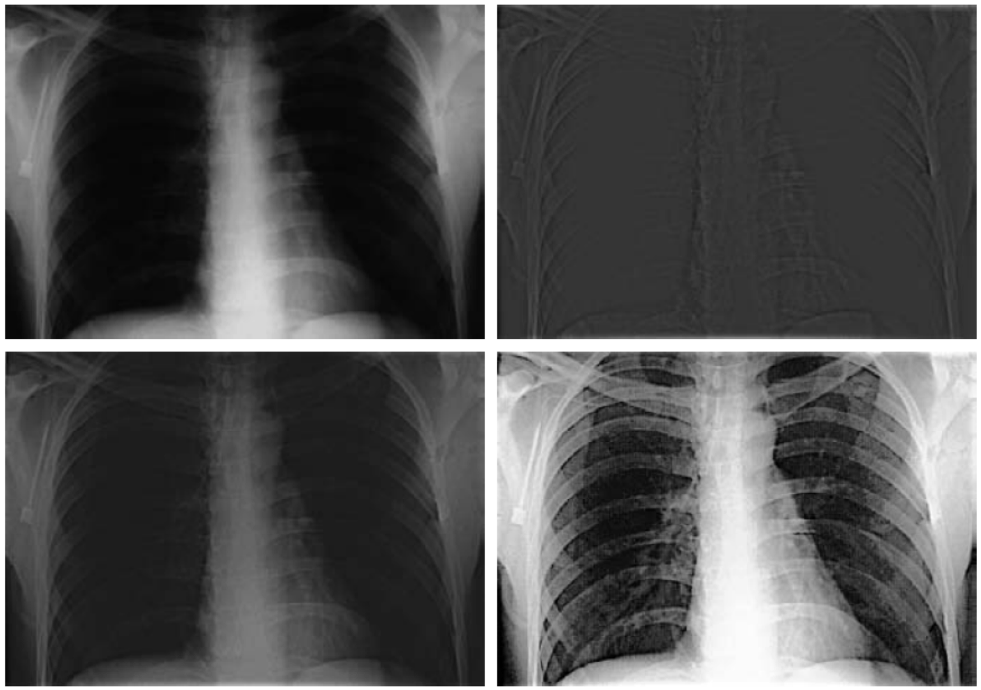

a b
c d

FIGURE 4.59 (a) A chest X-ray image. (b) Result of highpass filtering with a Gaussian filter. (c) Result of high-frequency-emphasis filtering using the same filter. (d) Result of performing histogram equalization on (c). (Original image courtesy of Dr. Thomas R. Gest, Division of Anatomical Sciences, University of Michigan Medical School.)

© 1992–2008 R. C. Gonzalez & R. E. Woods

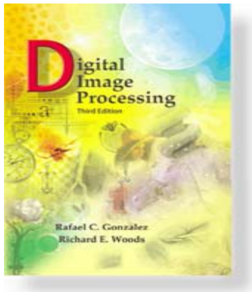

FIGURE 4.60 Summary of steps in homomorphic filtering.

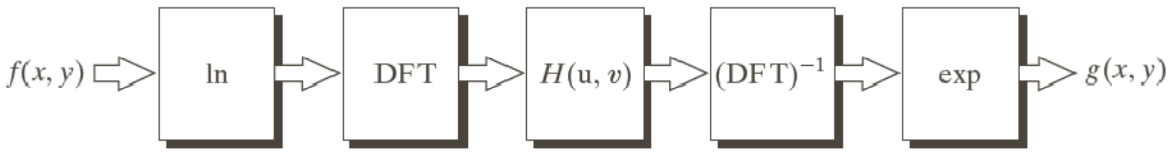

© 1992–2008 R. C. Gonzalez & R. E. Woods

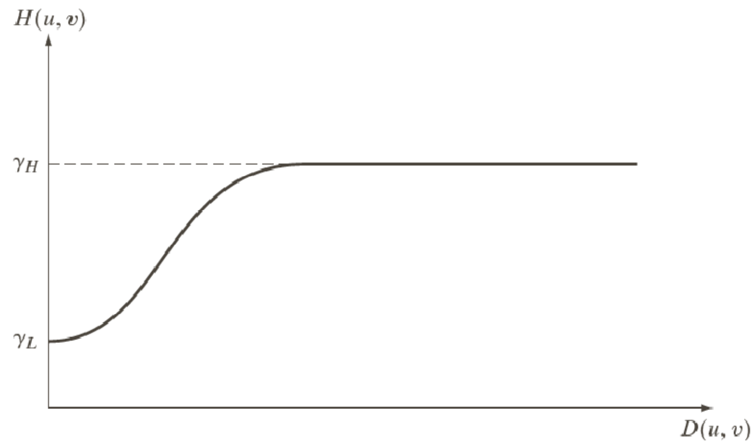

FIGURE 4.61 Radial cross section of a circularly symmetric homomorphic filter function. The vertical axis is at the center of the frequency rectangle and $D(u, v)$ is the distance from the center.

© 1992–2008 R. C. Gonzalez & R. E. Woods

Chapter 4
Filtering in the Frequency Domain

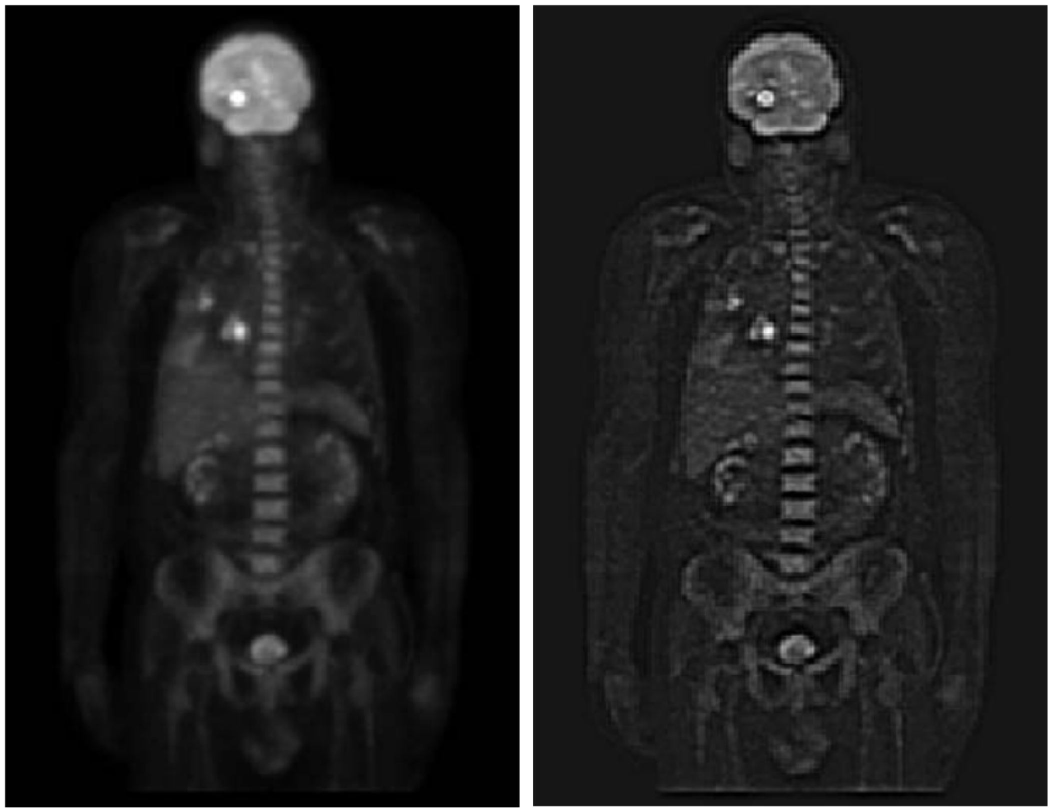

a b

FIGURE 4.62 (a) Full body PET scan. (b) Image enhanced using homomorphic filtering. (Original image courtesy of Dr. Michael E. Casey, CTI PET Systems.)

© 1992–2008 R. C. Gonzalez & R. E. Woods

TABLE 4.6
Bandreject filters. W is the width of the band, D is the distance $D(u, v)$ from the center of the filter, D_0 is the cutoff frequency, and n is the order of the Butterworth filter. We show D instead of $D(u, v)$ to simplify the notation in the table.

Ideal	Butterworth	Gaussian
$H(u,v) = \begin{cases} 0 & \text{if } D_0 - \frac{W}{2} \le D \le D_0 + \frac{W}{2} \\ 1 & \text{otherwise} \end{cases}$	$H(u,v) = \dfrac{1}{1 + \left[\dfrac{DW}{D^2 - D_0^2}\right]^{2n}}$	$H(u,v) = 1 - e^{-\left[\frac{D^2 - D_0^2}{DW}\right]^2}$

© 1992–2008 R. C. Gonzalez & R. E. Woods

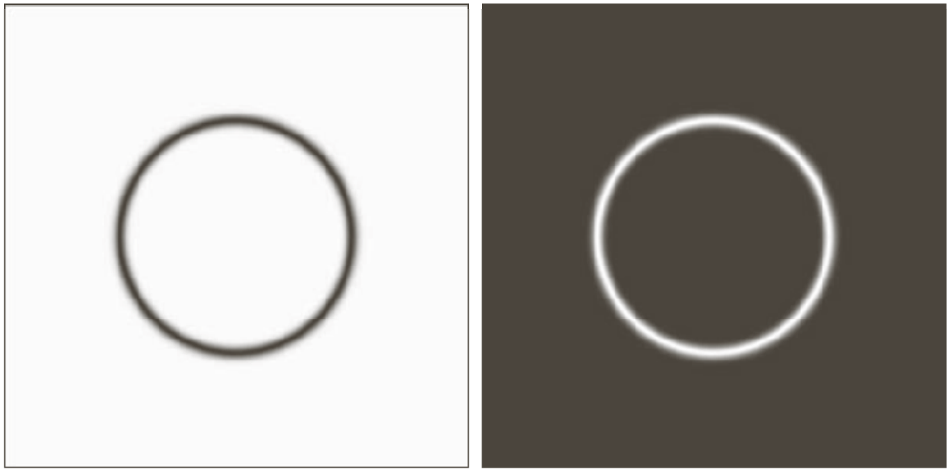

a b

FIGURE 4.63 (a) Bandreject Gaussian filter. (b) Corresponding bandpass filter. The thin black border in (a) was added for clarity; it is not part of the data.

© 1992–2008 R. C. Gonzalez & R. E. Woods

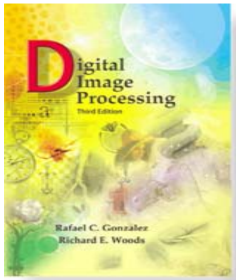

Chapter 4

Filtering in the Frequency Domain

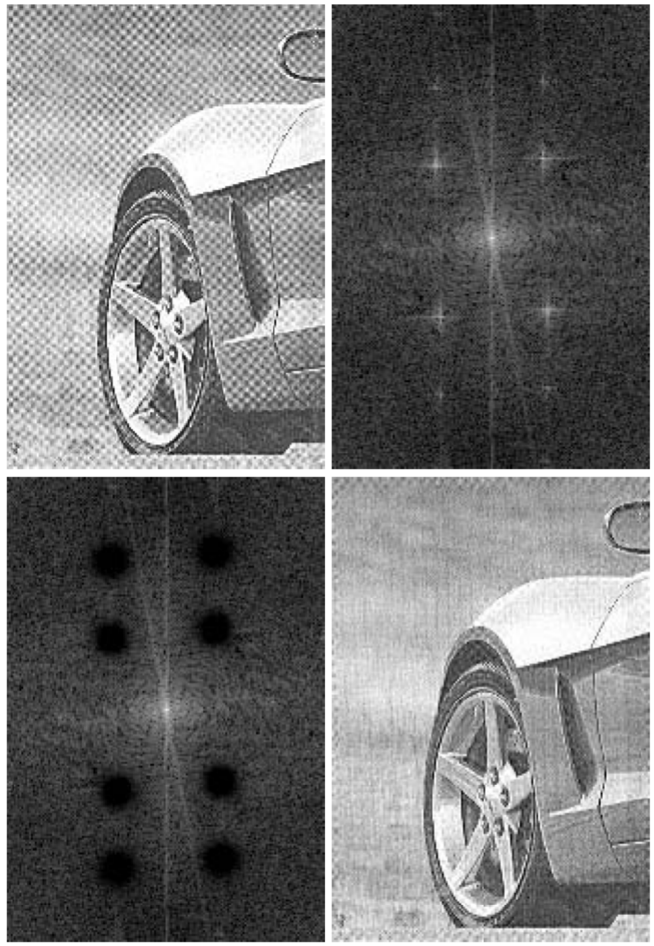

a b
c d

FIGURE 4.64
(a) Sampled newspaper image showing a moiré pattern. (b) Spectrum. (c) Butterworth notch reject filter multiplied by the Fourier transform. (d) Filtered image.

© 1992–2008 R. C. Gonzalez & R. E. Woods

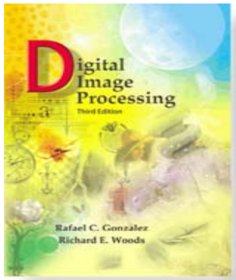

Chapter 4
Filtering in the Frequency Domain

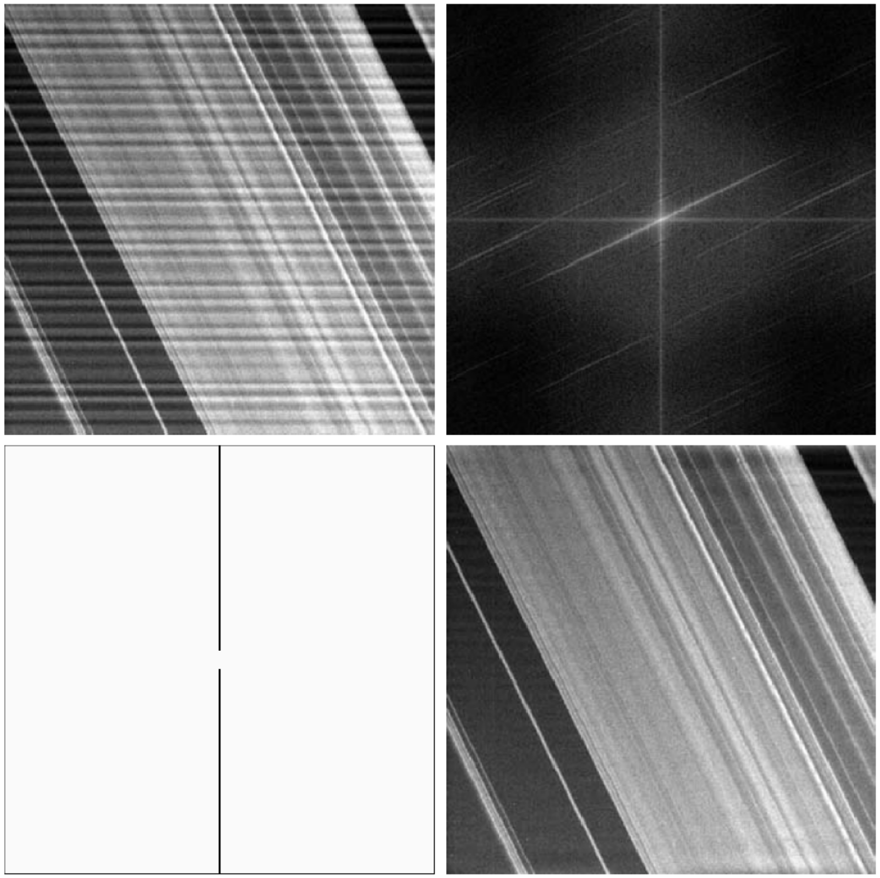

a b
c d

FIGURE 4.65
(a) 674 × 674 image of the Saturn rings showing nearly periodic interference. (b) Spectrum: The bursts of energy in the vertical axis near the origin correspond to the interference pattern. (c) A vertical notch reject filter. (d) Result of filtering. The thin black border in (c) was added for clarity; it is not part of the data. (Original image courtesy of Dr. Robert A. West, NASA/JPL.)

© 1992–2008 R. C. Gonzalez & R. E. Woods

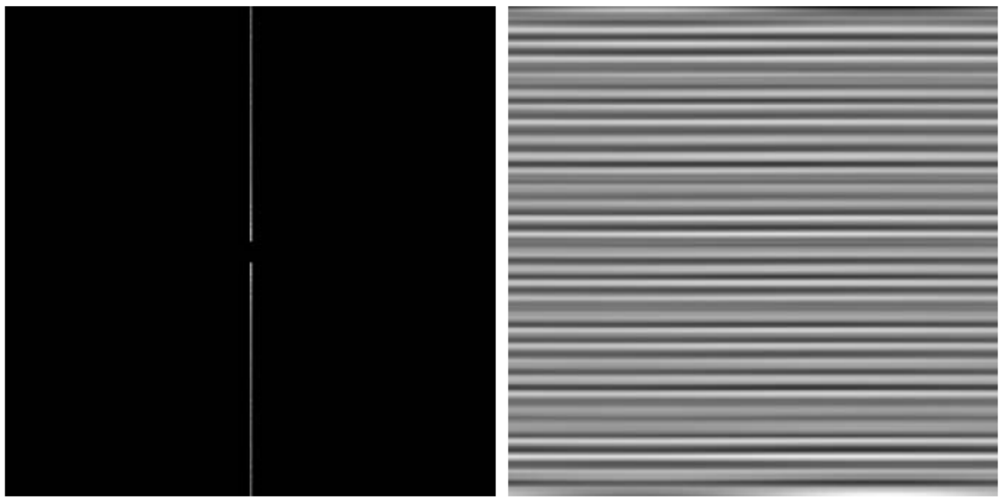

a b

FIGURE 4.66 (a) Result (spectrum) of applying a notch pass filter to the DFT of Fig. 4.65(a). (b) Spatial pattern obtained by computing the IDFT of (a).

© 1992–2008 R. C. Gonzalez & R. E. Woods

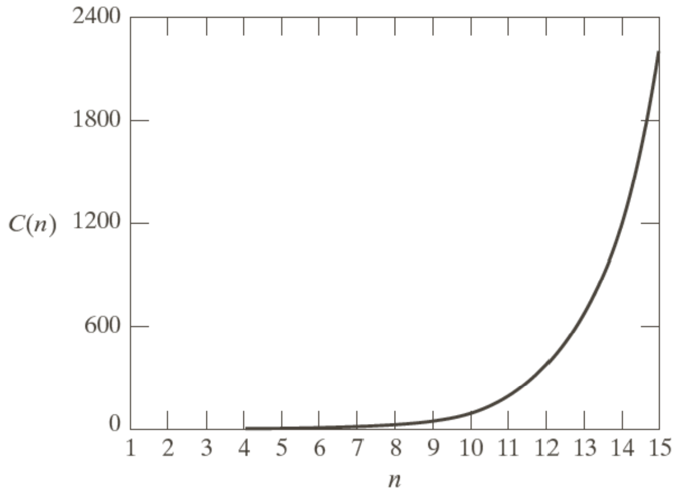

FIGURE 4.67 Computational advantage of the FFT over a direct implementation of the 1-D DFT. Note that the advantage increases rapidly as a function of n.

© 1992–2008 R. C. Gonzalez & R. E. Woods